

Pittsburg State University

## Pittsburg State University Digital Commons

---

Electronic Theses & Dissertations

---

Winter 12-13-2019

### FORMULATION OPTIMIZATION EFFECTS on MECHANICAL and RHEOLOGICAL PROPERTIES of FILLED POLYSILOXANES

Kevin McNay

Pittsburg State University, [kmcnay@gus.pittstate.edu](mailto:kmcnay@gus.pittstate.edu)

Follow this and additional works at: <https://digitalcommons.pittstate.edu/etd>



Part of the [Catalysis and Reaction Engineering Commons](#), and the [Polymer Science Commons](#)

---

#### Recommended Citation

McNay, Kevin, "FORMULATION OPTIMIZATION EFFECTS on MECHANICAL and RHEOLOGICAL PROPERTIES of FILLED POLYSILOXANES" (2019). *Electronic Theses & Dissertations*. 352.  
<https://digitalcommons.pittstate.edu/etd/352>

This Thesis is brought to you for free and open access by Pittsburg State University Digital Commons. It has been accepted for inclusion in Electronic Theses & Dissertations by an authorized administrator of Pittsburg State University Digital Commons. For more information, please contact [digitalcommons@pittstate.edu](mailto:digitalcommons@pittstate.edu).

FORMULATION OPTIMIZATION EFFECTS ON MECHANICAL AND  
RHEOLOGICAL PROPERTIES OF FILLED POLYSILOXANES

A Thesis Submitted to the Graduate School  
in Partial Fulfillment of the Requirements  
for the Degree of Master of Science

Kevin McNay

Pittsburg State University

Pittsburg, Kansas

December, 2019

FORMULATION OPTIMIZATION EFFECTS ON MECHANICAL AND  
RHEOLOGICAL PROPERTIES OF FILLED POLYSILOXANES

Kevin McNay

APPROVED:

Thesis Advisor

---

Dr. Jeanne H. Norton, The Department of Plastics Engineering Technology

Committee Member

---

Dr. Charles Neef, The Department of Chemistry

Committee Member

---

Mr. Paul Herring, The Department of Plastics Engineering Technology

## ACKNOWLEDGEMENTS

I would like to thank and express my great appreciation to my mentor and advisor, Dr. Jeanne H. Norton. Dr. Norton has been my professor, supervisor, mentor, advisor, and a friend to me throughout my college education. As my advisor, Dr. Norton has help me so much with regard to science and engineering, academics, research, and life. Dr. Norton's dedication to her work and students is truly inspiring and was an inspiration for my academic and career endeavors.

I would also like to acknowledge and thank my committee members: Dr. Charles Neef, and Mr. Paul Herring for their advice and encouragement towards my research. I would like to thank the Department of Chemistry and the Polymer Chemistry Initiative at Pittsburg State University for funding my position as a graduate research assistant. I am grateful for the faculty and staff, laboratory space, and equipment in the Department of Chemistry; the Kansas Polymer Research Center; and the Department of Plastics Engineering Technology at PSU.

Finally, I wish to thank my family and friends for their constant support and advice through my entire college career. Above all else, I would like to thank my wife, Emily McNay. She has given me never ending support through everything that I have done, whether it was financially, physically, or emotionally. I would like to dedicate this thesis to everyone mentioned above, because without these people, this thesis would not have been possible. Thank you!

# FORMULATION OPTIMIZATION EFFECTS ON MECHANICAL AND RHEOLOGICAL PROPERTIES OF FILLED POLYSILOXANES

An Abstract of the Thesis by  
Kevin McNay

Polysiloxanes are a class of high-performance polymeric materials that are used in a wide variety of applications, including O-rings, gaskets, sealants, coatings, and adhesives. These materials have high temperature resistances as well as flexibility at low temperatures. This is due to the bond between the oxygen and silicon atom, a bond that requires a high dissociation energy to break. However, their elastomers, which can be obtained by crosslinking linear precursors, generally exhibit low strength and have poor mechanical properties unless reinforced. Therefore, fillers, additives, UV-stabilizers, and anti-oxidants are often incorporated in order to improve the resulting properties.

The process of compounding incorporates additives into polysiloxane formulations, with one approach being twin-screw extrusion which vigorously mixes the additives into the polymer matrix. In this work, a lab-scale co-rotating twin-screw extruder was used to compound a commercially available reinforcing silica filler, Hi-Sil-233D, and a commercial polysiloxane, vinyl-terminated diphenyl-dimethyl siloxane copolymer (Gelest PDV-0535), to determine a filler ceiling loading. These copolymers were then compounded with two crosslinkers, trimethylsiloxane-terminated methylhydro-dimethyl siloxane copolymer (HMS-082 & HMS-151). The crosslinking reactions were initiated with two separate catalysts, platinum acetylacetonate in 1,3-dioxolane ( $\text{Pt}(\text{acac})_2$ ) and trimethyl(methylcyclopentadienyl) platinum IV in 1,3-dioxolane ( $((\text{MeCp})\text{Pt}(\text{Me})_3)$ ). In addition, diethyl azodicarboxylate (DEAD) in dry toluene was used

as a catalytic inhibitor. Finally, PDV-0535 with the  $\text{Pt}(\text{acac})_2$  catalyst is compounded in varied formulations and cured to analyze the shelf life and mechanical properties of the fully formulated system.

Thermogravimetric analysis (TGA) was used to determine the consistency of the additive content by analyzing the percent residue. Oscillatory rheometry was used to determine yield stress; and flow rheology was used to evaluate the thixotropy of the compounded samples. Rheometric analysis also helped determine the shelf-life of the polysiloxane system before becoming fully crosslinked. Soxhlet extraction was used to determine the gel content of the crosslinked systems. Dynamic mechanical analysis (DMA) was used to measure the mechanical properties of the fully cured polysiloxane formulations.

## TABLE OF CONTENTS

CHAPTER	PAGE
I. INTRODUCTION .....	1
1.1 Polysiloxanes .....	1
1.2 Fillers in polysiloxane elastomers.....	4
1.3 Vulcanization and crosslinking.....	8
1.4 Dynamic mechanical analysis.....	11
II. OBJECTIVES .....	15
2.1 Compounding polysiloxanes by twin-screw extrusion .....	15
2.2 Evaluation of filled model copolymer with different crosslinkers.....	16
III. EXPERIMENTAL .....	18
3.1 Materials .....	18
3.1.1 Commercial polysiloxane .....	18
3.1.2 Commercial filler.....	18
3.1.3 Commercial crosslinkers.....	18
3.2 Methods.....	19
3.2.1 Polysiloxane materials processing .....	19
3.2.1.1 Premixing silica-filled polysiloxanes.....	21
3.2.1.2 Compounding silica-filled polysiloxanes .....	21
3.3 Characterization methods.....	21
3.3.1 Thermal characterization by thermogravimetric analysis.....	21
3.3.2 Rheological characterization.....	22
3.3.2.1 Oscillatory rheometry .....	22
3.3.2.2 Flow rheology .....	22
3.3.3 Material curing.....	22
3.3.3.1 Dark curing for shelf stability determination.....	22
3.3.3.2 UV curing .....	23
3.3.4 Cured material analysis.....	23
3.3.4.1 Soxhlet extraction of vulcanized samples .....	23
3.3.4.2 Dynamic mechanical analysis of vulcanized samples .....	24
IV. RESULTS AND DISCUSSION.....	26
COMPARISON OF CATALYST TYPES IN FILLED SYSTEMS .....	26
4.1 Observations of commercial polysiloxane, filler, crosslinkers, catalyst, inhibitor, and compounded material.....	26
4.1.1 Observations of commercial polysiloxane.....	26
4.1.2 Observations of commercial filler .....	26
4.1.3 Observations of commercial crosslinkers .....	27
4.1.4 Observations of catalysis and inhibitor.....	27
4.1.5 Observations of filled compound material.....	28
4.2 Formulation of filled commercial polysiloxanes to compare catalyst types .....	28
4.3 Thermogravimetric analysis of commercial polysiloxanes.....	28
4.3.1 Thermogravimetric analysis of filled (MeCp)Pt(Me) <sub>3</sub> samples .....	29
4.3.2 Thermogravimetric analysis of filled Pt(acac) <sub>2</sub> samples.....	33
4.4 Oscillatory rheometry of filled commercial polysiloxanes .....	35
4.4.1 Oscillatory rheometry of filled (MeCp)Pt(Me) <sub>3</sub> samples.....	36
4.4.2 Oscillatory rheometry of filled Pt(acac) <sub>2</sub> samples.....	36
4.5 Flow rheology of filled commercial polysiloxanes.....	37
4.5.1 Flow rheology of filled (MeCp)Pt(Me) <sub>3</sub> Samples .....	38

4.5.2 Flow rheology of filled Pt(acac) <sub>2</sub> samples .....	39
4.6 Summary .....	42
V. RESULTS AND DISCUSSION .....	43
COMPARISON OF CATALYST AND INHIBITOR LEVELS.....	43
5.1 Formulation modifications to extend shelf life .....	43
5.2 Observations of filled model copolymer .....	44
5.3 Thermogravimetric analysis of filled model copolymer .....	44
5.4 Oscillatory rheometry of filled commercial copolymer.....	53
VI. CONCLUSION.....	68
6.1 Future work.....	71
REFERENCES .....	74



## LIST OF TABLES

TABLE	PAGE
<b>Table 1.</b> Glass transition temperatures of common polysiloxanes. <sup>1</sup> .....	4
<b>Table 2.</b> Formulations details. ....	28
<b>Table 3.</b> Thermal properties of filled PDV-0535 compounded with 28 wt% Hi-Sil-233D filler, HMS-082 crosslinker, (MeCp)Pt(Me) <sub>3</sub> catalyst and DEAD inhibitor as crosslinking occurs. ....	30
<b>Table 4.</b> Thermal properties of the filled PDV-0535 compounded with 28 wt% Hi-Sil-233D filler, HMS-15 crosslinker, (MeCp)Pt(Me) <sub>3</sub> catalyst and DEAD inhibitor as crosslinking occurs. ....	32
<b>Table 5.</b> Thermal properties of the filled PDV-0535 compounded with 28 wt% Hi-Sil-233D filler, HMS-082 crosslinker, Pt(acac) <sub>2</sub> catalyst and DEAD inhibitor as crosslinking occurs. ....	33
<b>Table 6.</b> Thermal properties of the filled PDV-0535 compounded with 28 wt% Hi-Sil-233D filler, HMS-151 crosslinker, Pt(acac) <sub>2</sub> catalyst and DEAD inhibitor as crosslinking occurs. ....	34
<b>Table 7.</b> Yield stress of filled PDV-0535 compounded with 28 wt% Hi-Sil-233D filler, HMS-082 crosslinker, (MeCp)Pt(Me) <sub>3</sub> catalysis and DEAD inhibitor as crosslinking occurred over time. ...	36
<b>Table 8.</b> Yield stress of the filled PDV-0535 compounded with 28 wt% Hi-Sil-233D filler, HMS-151 crosslinker, (MeCp)Pt(Me) <sub>3</sub> catalysis and DEAD inhibitor as crosslinking occurs over time. ....	36
<b>Table 9.</b> Yield stress of filled PDV-0535 compounded with 28 wt% Hi-Sil-233D filler, HMS-082 crosslinker, Pt(acac) <sub>2</sub> catalysis and DEAD inhibitor as crosslinking occurred over time. ....	37
<b>Table 10.</b> Yield stress of filled PDV-0535 compounded with 28 wt% Hi-Sil-233D filler, HMS-151 crosslinker, Pt(acac) <sub>2</sub> catalysis and DEAD inhibitor as crosslinking occurred over time. ....	37
<b>Table 11.</b> Formulations details. ....	44
<b>Table 12.</b> Thermal properties of filled PDV-0535 compounded with 28 wt% Hi-Sil-233D filler, HMS-151 crosslinker, Pt(acac) <sub>2</sub> (250ppm) catalysis and DEAD (1:4) inhibitor as crosslinking occurred. ....	46
<b>Table 13.</b> Thermal properties of filled PDV-0535 compounded with 28 wt% Hi-Sil-233D filler, HMS-151 crosslinker, Pt(acac) <sub>2</sub> (250ppm) catalysis and DEAD (1:2) inhibitor as crosslinking occurred. ....	47

<b>Table 14.</b> Thermal properties of filled PDV-0535 compounded with 28 wt% Hi-Sil-233D filler, HMS-151 crosslinker, Pt(acac) <sub>2</sub> (125ppm) catalysis and DEAD (1:4) inhibitor as crosslinking occurred. ....	48
<b>Table 15.</b> Thermal properties of filled PDV-0535 compounded with 28 wt% Hi-Sil-233D filler, HMS-151 crosslinker, Pt(acac) <sub>2</sub> (125ppm) catalysis and DEAD (1:2) inhibitor as crosslinking occurred. ....	49
<b>Table 16.</b> Thermal properties of filled PDV-0535 compounded with 28 wt% Hi-Sil-233D filler, HMS-082 crosslinker, Pt(acac) <sub>2</sub> (250ppm) catalysis and DEAD (1:4) inhibitor as crosslinking occurred. ....	50
<b>Table 17.</b> Thermal properties of filled PDV-0535 compounded with 28 wt% Hi-Sil-233D filler, HMS-082 crosslinker, Pt(acac) <sub>2</sub> (250ppm) catalysis and DEAD (1:2) inhibitor as crosslinking occurred. ....	51
<b>Table 18.</b> Thermal properties of filled PDV-0535 compounded with 28 wt% Hi-Sil-233D filler, HMS-082 crosslinker, Pt(acac) <sub>2</sub> (125ppm) catalysis and DEAD (1:4) inhibitor as crosslinking occurred. ....	52
<b>Table 19.</b> Thermal properties of the filled PDV-0535 compounded with 28 wt% Hi-Sil-233D filler, HMS-082 crosslinker, Pt(acac) <sub>2</sub> (125ppm) catalysis and DEAD (1:2) inhibitor as crosslinking occurred. ....	53
<b>Table 20.</b> Yield stress of filled model copolymer compounded with HMS-151, Pt(acac) <sub>2</sub> (250ppm) and DEAD (1:4) each day until crosslinked.....	54
<b>Table 21.</b> Yield stress of filled model copolymer compounded with HMS-151, Pt(acac) <sub>2</sub> (250ppm) and DEAD (1:2) each day until crosslinked.....	54
<b>Table 22.</b> Yield stress of filled model copolymer compounded with HMS-151, Pt(acac) <sub>2</sub> (125ppm) and DEAD (1:4) each day until crosslinked.....	55
<b>Table 23.</b> Yield stress of filled model copolymer compounded with HMS-151, Pt(acac) <sub>2</sub> (125ppm) and DEAD (1:2) each day until crosslinked.....	55
<b>Table 24.</b> Yield stress of filled model copolymer compounded with HMS-082, Pt(acac) <sub>2</sub> (250ppm) and DEAD (1:4) each day until crosslinked.....	56
<b>Table 25.</b> Yield stress of filled model copolymer compounded with HMS-082, Pt(acac) <sub>2</sub> (250ppm) and DEAD (1:2) each day until crosslinked.....	56
<b>Table 26.</b> Yield stress of filled model copolymer compounded with HMS-082, Pt(acac) <sub>2</sub> (125ppm) and DEAD (1:4) each day until crosslinked.....	57
<b>Table 27.</b> Yield stress of the filled model copolymer compounded with HMS-082, Pt(acac) <sub>2</sub> (125ppm) and DEAD (1:2) each day until crosslinked.....	57

<b>Table 28.</b> Percent of crosslinking of the filled model copolymer compounded with HMS-151 crosslinker.....	64
<b>Table 29.</b> Percent of crosslinking of the filled model copolymer compounded with HMS-082 crosslinker.....	65
<b>Table 30.</b> Onset temperature and $\tan \delta$ of HMS-151 systems.....	66
<b>Table 31.</b> Onset temperature and $\tan \delta$ of HMS-082 systems.....	66

## LIST OF FIGURES

FIGURE	PAGE
<b>Figure 1.</b> General structure of (a) siloxane bond, (b) silicon dioxide, (c) silicate ion.....	2
<b>Figure 2.</b> Comparison structures of (a) siloxane bond and (b) silicon-carbon bond with their respective bond lengths and bond angles .....	3
<b>Figure 3.</b> Silanol groups on the surface of silica: (a) isolated silanols, (b) geminal silanols, and (c) vicinal-bridged silanols. Also shown: adsorbed water.....	5
<b>Figure 4.</b> Interaction of a surface silanol group of a silica particle and the polymer backbone.....	6
<b>Figure 5.</b> Aggregated structure of silica particles with silanol groups.....	6
<b>Figure 6.</b> Filler network structure comprised of aggregates and agglomerates.....	7
<b>Figure 7.</b> Graph representing crosslinking as a function of time and viscosity. ....	9
<b>Figure 8.</b> Viscosity vs. time at different curing temperatures: 1) standard temperature, 2) increased temperature, 3) decreased temperature, 4) temperature below reaction activation temperature .....	10
<b>Figure 9.</b> Hydrosilylation reaction with platinum catalysis .....	11
<b>Figure 10.</b> Examples of different DMA stages for different analytical techniques. Tension, compression, cantilever clamping for flexural analysis, and shear sandwich clamping (left to right).....	12
<b>Figure 11.</b> Typical stress/strain curve generated by DMA.....	13
<b>Figure 12.</b> Thermo Fisher Scientific Process 11 twin-screw extruder. ....	20
<b>Figure 13.</b> 3mm aluminum mold for UV curing of elastomers. 0.5mm mold is not shown. ....	23
<b>Figure 14.</b> Soxhlet extraction apparatus.....	24
<b>Figure 15.</b> Dynamic mechanical analysis shear sandwich stage. ....	25
<b>Figure 16.</b> Appearance of the commercial polysiloxane PDV-0535. ....	26
<b>Figure 17.</b> Appearance of the commercial filler: Hi-Sil-233D. ....	27
<b>Figure 18.</b> Appearance of the commercial crosslinker HMS-082. HMS-151 is not shown.....	27

<b>Figure 19.</b> Appearance of the catalysts and inhibitor: Pt(acac) <sub>2</sub> , DEAD (left to right). (MeCp)Pt(Me) <sub>3</sub> is not shown .....	27
<b>Figure 20.</b> Appearance of the filled model copolymer compounded material. ....	28
<b>Figure 21.</b> Back-biting depolymerization mechanism during thermal decomposition. ....	29
<b>Figure 22.</b> TGA thermograms of filled PDV-0535 compounded with 28 wt% Hi-Sil-233D filler, HMS-082 crosslinker, (MeCp)Pt(Me) <sub>3</sub> catalyst and DEAD inhibitor over time. Day 0 (—), Day 1 – Run 1 (—), Day 1 – Run 2 (—), Day 1 – Run 3 (—). ....	30
<b>Figure 23.</b> TGA thermograms of the filled PDV-0535 compounded with 28 wt% Hi-Sil-233D filler, HMS-151 crosslinker, (MeCp)Pt(Me) <sub>3</sub> catalyst and DEAD inhibitor over time. Day 0-Run 1 (—), Day 1-Run 1 (—).....	32
<b>Figure 24.</b> TGA thermograms of the filled PDV-0535 compounded with 28 wt% Hi-Sil-233D filler, HMS-082 crosslinker, Pt(acac) <sub>2</sub> catalyst and DEAD inhibitor over time. Day 0 (—), Day 1 (—), Day 2 (—), and Day 3 (—).....	33
<b>Figure 25.</b> TGA thermograms of the filled PDV-0535 compounded with 28 wt% Hi-Sil-233D filler, HMS-151 crosslinker, Pt(acac) <sub>2</sub> catalyst and DEAD inhibitor as crosslinking occurs: Day 0 (—), Day 1 (—), Day 2 (—), and Day 3 (—). ....	34
<b>Figure 26.</b> Storage and loss modulus versus oscillatory stress for a typical filled material. Yield stress is determined by the point where the G' (●) and G'' (●) curves intersect.....	35
<b>Figure 27.</b> Deconstruction and reconstruction of polymer network. <sup>17</sup> .....	38
<b>Figure 28.</b> Thixotropic loops of flow rheology analysis filled PDV-0535 materials compounded with crosslinkers and (MeCp)Pt(Me) <sub>3</sub> :HMS-082 Day 0 (●), HMS-082 Day1 (●), and HMS-151 Day 1 (●). ....	38
<b>Figure 29.</b> Thixotropic loops of flow rheology analysis filled material with HMS-082 and Pt(acac) <sub>2</sub> : Day 0 (●), Day 1 (●), Day 2 (●), and Day 3 (●).....	39
<b>Figure 30.</b> Thixotropic loops of flow rheology analysis for filled material with HMS-151 and Pt(acac) <sub>2</sub> : Day 0 (●), Day 1 (●), Day 2 (●), and Day 3 (●).....	41
<b>Figure 31.</b> Appearance of the filled model copolymer compounded material. ....	44
<b>Figure 32.</b> TGA thermograms of filled model copolymer compounded with HMS-151, Pt(acac) <sub>2</sub> (250ppm), and DEAD(1:4): Day 0 (—), and Day 1 (—). ....	45
<b>Figure 33.</b> TGA thermograms of filled model copolymer compounded with HMS-151, Pt(acac) <sub>2</sub> (250ppm), and DEAD (1:2): Day 0 (—), Day 1 (—), and Day 2 (—). ....	47
<b>Figure 34.</b> TGA thermograms of filled model copolymer compounded with HMS-151, Pt(acac) <sub>2</sub> (125ppm), and DEAD (1:4): Day 0 (—), Day 1 (—), and Day 2 (—). ....	48

<b>Figure 35.</b> TGA thermograms of filled model copolymer compounded with HMS-151, Pt(acac) <sub>2</sub> (125ppm), and DEAD (1:2): Day 0 (—), Day 1 (—), Day 2 (—), Day 3 (—), and Day 4 (—)....	49
<b>Figure 36.</b> TGA thermograms of filled model copolymer compounded with HMS-082, Pt(acac) <sub>2</sub> (250ppm), and DEAD (1:4): Day 0 (—), Day 1 (—), Day 2 (—), Day 3 (—).....	50
<b>Figure 37.</b> TGA thermograms of filled model copolymer compounded with HMS-082, Pt(acac) <sub>2</sub> (250ppm), and DEAD (1:2): Day 0 (—), Day 1 (—), and Day 2 (—). ....	51
<b>Figure 38.</b> TGA thermograms of filled model copolymer compounded with HMS-082, Pt(acac) <sub>2</sub> (125ppm), and DEAD (1:4): Day 0 (—), Day 1 (—), and Day 2 (—). ....	52
<b>Figure 39.</b> TGA thermograms of the filled model copolymer compounded with HMS-082, Pt(acac) <sub>2</sub> (125ppm), and DEAD (1:2): Day 0 (—), Day 1 (—), Day 2 (—), Day 3 (—), and Day 4 (—).....	53
<b>Figure 40.</b> Thixotropic loops of the flow rheology for the reference silicone compared to the filled model copolymer materials compounded with HMS-151, Pt(acac) <sub>2</sub> (250ppm), and DEAD (1:4): Day 0 (●), and Day 1 (●).....	58
<b>Figure 41.</b> Thixotropic loops of the flow rheology for the reference silicone compared to the filled model copolymer materials compounded with HMS-151, Pt(acac) <sub>2</sub> (250ppm), and DEAD (1:2): Day 0 (●), Day 1 (●), and Day 2 (●). ....	59
<b>Figure 42.</b> Thixotropic loops of the flow rheology analysis for the reference silicone compared to the filled model copolymer materials compounded with HMS-151, Pt(acac) <sub>2</sub> (125ppm), and DEAD (1:4): Day 0 (●), Day 1 (●), and Day 2 (●). ....	59
<b>Figure 43.</b> Thixotropic loops of the flow rheology analysis for the reference silicone compared to the filled model copolymer materials compounded with HMS-151, Pt(acac) <sub>2</sub> (125ppm), and DEAD (1:2): Day 0 (●), Day 1 (●), Day 2 (●), Day 3 (●), and Day 4 (●). ....	60
<b>Figure 44.</b> Thixotropic loops of the flow rheology analysis for the reference silicone compared to the filled model copolymer materials compounded with HMS-082, Pt(acac) <sub>2</sub> (250ppm), and DEAD (1:4): Day 0 (●), Day 1 (●), Day 2 (●), and Day 3 (●). ....	61
<b>Figure 45.</b> Thixotropic loops of the flow rheology analysis for the reference silicone compared to the filled model copolymer materials compounded with HMS-082, Pt(acac) <sub>2</sub> (250ppm), and DEAD (1:2): Day 0 (●), Day 1 (●), and Day 2 (●). ....	62
<b>Figure 46.</b> Thixotropic loops of the flow rheology analysis for the reference silicone compared to the filled model copolymer materials compounded with HMS-082, Pt(acac) <sub>2</sub> (125ppm), and DEAD (1:4): Day 0 (●), Day 1 (●), and Day 2 (●). ....	63
<b>Figure 47.</b> Thixotropic loops of the flow rheology analysis for the reference silicone compared to the filled model copolymer materials compounded with HMS-082, Pt(acac) <sub>2</sub> (125ppm), and DEAD (1:2): Day 0 (●), Day 1 (●), Day 2 (●), Day 3 (●), and Day 4 (●). ....	63

## LIST OF ABBREVIATIONS

$\mu\text{m}$  – Micrometer

$\text{\AA}$  – Angstrom

DSC – Differential scanning calorimetry

DMA – Dynamic mechanical analysis

$\gamma$  – Gamma

J – Joules

Hz – Hertz

L:D ratio – Length to diameter ratio

$\text{m}^2/\text{g}$  – Meters squared per gram

mm – Millimeter

PDMS – Polydimethylsiloxane

sec – second

$\sigma$  – Sigma

$T_g$  – Glass transition temperature

TGA – Thermogravimetric analysis

wt% – Weight percent

## CHAPTER I

### 1. INTRODUCTION

#### 1.1 Polysiloxanes

Polysiloxane elastomers are some of the most unique elastomeric materials due to properties including high temperature resistance and flexibility at low temperatures. Natural rubber has an upper use temperature of 80°C and a glass transition temperature ( $T_g$ ) at -72°C. In contrast, polydimethylsiloxane (PDMS) has an upper use temperature of 400°C and a  $T_g$  of -123°C.<sup>1,2</sup> These properties allow polysiloxane materials to be viable for a wide range of applications, such as O-rings, sealants, coatings, and adhesives in harsh environments.<sup>1</sup>

Polysiloxanes are the most common and one of the most important organosilicon polymers used in polymer chemistry.<sup>3</sup> The primary structure of the polymer is a siloxane bond (Si-O) that is comprised of alternating silicon and oxygen atoms in long polymeric chains. Every silicon atom on this chain carries two functional groups. Silicon is found in Group IVA of the periodic table and is the most abundant of those elements. The earth's crust contains 27% of silicon by mass. In nature, silicon is seldom found by itself and is usually bonded to oxygen to form silicon dioxide ( $\text{SiO}_2$  or  $\text{SiO}_4$ ).<sup>3,4</sup> Figure 1<sup>1</sup> shows the general structure of siloxane bond, silicon dioxide, and the silicate ion.



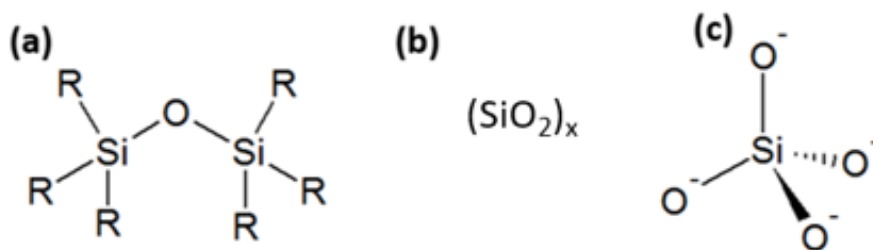


**Figure 1.** General structure of (a) siloxane bond, (b) silicon dioxide, (c) silicate ion.<sup>1</sup>

Polysiloxanes possess many impressive properties such as flexibility at extreme temperature, low surface energy, high temperature stability, and high permeability to gasses. These polymers have extreme flexibility at broad temperatures because of their low  $T_g$ s, some of the lowest of polymer science materials. Polysiloxanes achieve their flexibility because of the wide range of possible bond angles of the siloxane bond. High temperature stability is also attributed to the siloxane bond. Finally, the low surface energy of polysiloxane allows these polymers to be hydrophobic and appropriate for non-stick surfaces.<sup>3</sup>

The siloxane bond contains partial ionic and partial double bond characteristics. This characteristic is attributed to the difference in electronegativity of silicon and oxygen.<sup>1,5</sup> The partial double bond is attributed to the overlapping of the  $p$  orbitals in the oxygen atom with the low-energy  $d$  orbitals in the silicon atom. The difference in size between the oxygen and silicon atoms allows the oxygen atom to back-donate its lone electron pair to create the partial double bond instead of a single bond. The partial double bond, coupled with the partial ionic characteristic, result in the high temperature properties of polysiloxanes.<sup>1</sup> The bond between silicon and oxygen contains a high degree of strength and is considerably stronger than a carbon-oxygen bond. The energy required to break a carbon-oxygen bond is roughly 85.5 kcal/mol while a siloxane bond possesses a breaking point at 106 kcal/mol. The higher bond strength is attributed to the

increasing amount of ionic character in chemical bonds according to Dvornic and coworkers.<sup>1</sup> In addition to the ionic character of the siloxane bond, the partial double bond is created by the back-donating oxygen atom contributes to the strength of the siloxane bond. It is generally more difficult to break a double bond than a single bond.<sup>1</sup>

The partial double bond character is further supported by the length of the polysiloxane bond. The average length of a polysiloxane bond length is between 1.63 Å to 1.66 Å. This length is shorter than single bond between silicon and oxygen, which is estimated to be 1.83 Å. The attractive forces between the silicon and oxygen allow the bond to be stronger than expected with a partial double bond characteristic.<sup>1</sup> Figure 2<sup>6</sup> displays the comparison between a siloxane bond and a silicon-carbon bond.

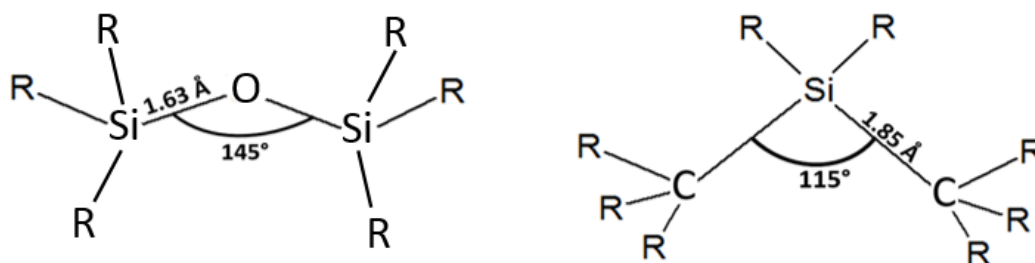


**Figure 2.** Comparison structures of (a) siloxane bond and (b) silicon-carbon bond with their respective bond lengths and bond angles.<sup>6</sup>

The bond also provides the ability for these materials to be flexible at low temperatures. The standard bond angle in a single bond C-Si-C (carbon silicon bond), measures between 106° and 118°. The bond angle in a siloxane bond can vary between 104° to 180°, with 144° to 150° being the most widely reported. These measurements demonstrate a range of stable bond angles associated with the siloxane bond and show that the bond angle can increase to allow the two silicon atom to rotate freely around the common oxygen atom. This allows the siloxane bond to be highly deformable. Figure 2 compares the bond angles between a siloxane bond and a silicon-carbon bond.<sup>4</sup> The  $T_g$  of

polysiloxanes also play a part in the flexibility of these polymers; polysiloxanes have the lowest  $T_g$  in polymer science.<sup>1</sup> Table 1 displays the glass transition temperatures of common polysiloxanes.<sup>1</sup>

**Table 1.** Glass transition temperatures of common polysiloxanes.<sup>1</sup>

<b>Polymer</b>	<b><math>T_g</math> (°C)</b>
Natural Rubber	-72
Polymethylphenylsiloxane	-28
Poly(diphenyl-co-dimethyl) (30:70 mol%)	-64
Polydimethylsiloxane	-123
Polymethylethylsiloxane	-135
Polydiethylsiloxane	-139

## **1.2 Fillers in polysiloxane elastomers**

Polysiloxane elastomers by themselves exhibit low strength and poor mechanical properties. Additives, such as fillers and stabilizers, are incorporated to elastomeric materials to enhance the mechanical properties and produce practical materials for production. Without fillers, polysiloxane materials would be very weak and would not be practical for commercial applications.<sup>1</sup>

Fillers are divided into two categories: extending fillers and reinforcing fillers. Extending fillers are considered non- to semi-reinforcing fillers. Extending fillers are used to reduce cost by “extending” the formulation of the polymeric resin.<sup>7</sup> Reinforcing fillers, on the other hand, are used to improve mechanical properties when compared to unfilled material.<sup>8,9</sup> Reinforcing fillers can further be separated into inactive and active fillers. Inactive fillers are usually added to the elastomers for economic purposes and do little to improve material properties. Active fillers include chemically-treated silica fillers that considerably improve physical properties such as tensile strength, abrasion resistance, and heat aging characteristics.

Active reinforcing silica can be further separated into fumed and precipitated fillers. Fumed silica is the purest form of synthetic silica that is available commercially at 99.8% silica.<sup>10</sup> Fumed silica filler is manufactured by hydrolysis of chlorosilane, such as silicon tetrachloride that is burned in an oxygen and hydrogen flame through a pyrogenic process. When fumed silica is produced, hydroxyl groups on the surface of the particles create a hydrophilic surface that can be used in hydrogen bonding with the polysiloxane backbone. Fumed silica particles are generally smaller than precipitated silica particles and have a higher surface area.<sup>11</sup> Precipitated silica is produced from the reaction of a mineral acid with an alkaline silicate solution. This solution, with the addition of water, are agitated until precipitation occurs. The porosity and particle size are determined by the speed of agitation, the duration of the reaction, the amount of reactants, along with temperature, concentration, and pH of the reactions. The particles are filtered and washed to eliminate salt byproduct and then dried to remove moisture. Precipitated silicas are generally less pure than fumed silica fillers at 93 – 95% silica.<sup>11</sup>

Silica fillers have active hydroxyl groups that can attach to the silicon atom to form silanol groups. The silanol groups in shown Figure 3 are divided in three groups: isolated single silanols, geminal silanediols, and vicinal-bridged silanols.<sup>12</sup>

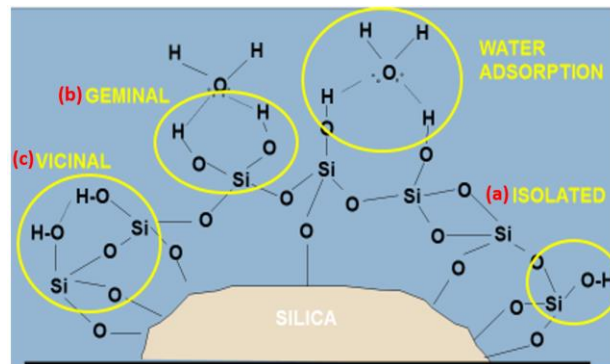


**Figure 3.** Silanol groups on the surface of silica: (a) isolated silanols, (b) geminal silanols, and (c) vicinal-bridged silanols. Also shown: adsorbed water.<sup>13</sup>

The surface silanol groups of the fillers provide many functions, but one in particular is the interaction between the silanol group and the polysiloxane backbone. The polymer chains become adsorbed on the surface of the silica due to the wetting of the filler by the polymer.<sup>14,15</sup> This interaction limits the mobility of the polymer chain, thereby reinforcing and improving the filled material's mechanical properties and thermal stability.<sup>9,16</sup> The interaction between the silica particle and polysiloxane backbone can be seen in Figure 4.<sup>17</sup>

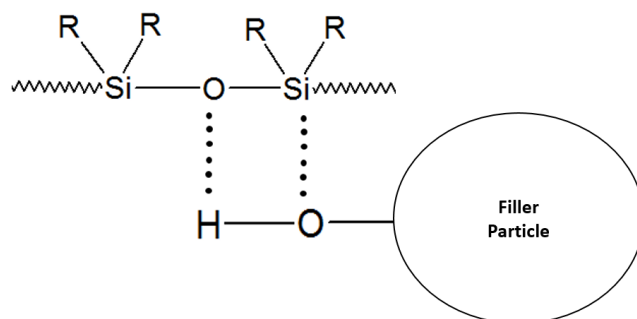


**Figure 4.** Interaction of a surface silanol group of a silica particle and the polymer backbone.

The surface of a silica particle can also interact with other silica particles through a process called aggregation. Aggregation occurs as a result of the high surface area of filler particles and generally happens during production and compounding. The abundance of the silanol groups leads to aggregated three-dimensional structures through hydrogen bonding.<sup>15,18-20</sup> Figure 5 displays an aggregated network of silica particle.<sup>21</sup>

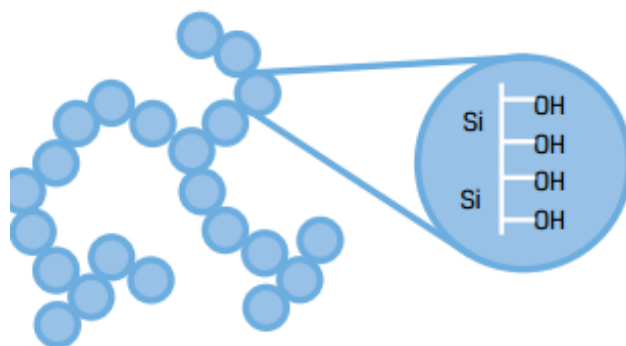


**Figure 5.** Aggregated structure of silica particles with silanol groups.<sup>21</sup>

The association of silica aggregates with the polymer backbone can improve the mechanical, thermal, and rheological properties of the material. The filler structure can interrupt the release of volatiles during thermal decomposition, thereby enhancing thermal stability. The increased hydrogen-bonding interactions with the polysiloxane backbone enhances mechanical properties. Lastly, the aggregated network hinders the mobility of the polymer chain, thus enhancing the rheological properties.<sup>18,20,22-32</sup>

Filler aggregation can also be detrimental to material properties at higher levels. Since the silica particles can interact with each other, clusters of aggregated networks can continue to interact with other networks to form agglomerates. Figure 6 shows the comparison between aggregated networks and agglomerated networks.<sup>33</sup> Agglomerates can happen because of a lack of filler distribution in the polymer matrix as well as the filler interacting with itself instead of the polymer.<sup>1,34,35</sup> This can lead to diminished mechanical and rheological properties because of the lack of interaction between the polymer backbone and the filler.<sup>18,20,26,36-39</sup>

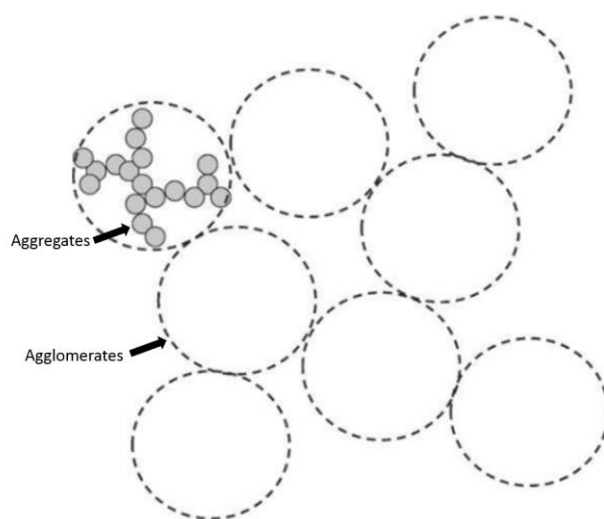


**Figure 6.** Filler network structure comprised of aggregates and agglomerates.<sup>33</sup>

Filled polysiloxane elastomers are used in a variety of industries for many different applications. These applications are usually subjected to extreme temperatures

over a long period of time. The most common applications are O-rings, gaskets, and sealants for the military, automotive, and aircraft/aerospace industries. These products include belts for conveyor lines, engine and transmission seals, door seals for aircraft and oven doors, and protective coatings for jets, rockets, and submarines.<sup>1</sup>

### **1.3 Vulcanization and crosslinking**

In addition to the incorporation of fillers, the mechanical properties of elastomers can be enhanced through the process of vulcanization, or the crosslinking, of rubber. The crosslinks contribute to the elastomeric properties by preventing the individual polymer chains from slipping past each other, even when heated. However, because the crosslinks are permanent bonds, if excessive heat and extreme stresses are applied to the crosslinked elastomers, the crosslinks will break and are unable to be reformed, which results in material degradation.<sup>40</sup>

Vulcanization was first discovered by Charles Goodyear in the mid 1800's. Goodyear, a largely unsuccessful inventor, had been working for his father's hardware store when he became interested in rubbers. Goodyear spent years trying to develop a method to curing natural rubber so that it would lose its adhesiveness when warm and brittleness when cold.<sup>41</sup> He discovered the non-stick rubber in 1839, when he accidentally heated sulfur-treated rubber on a stove. Sulfur created covalent crosslinks between the polyisoprene chains to create a non-sticky, flexible material.

The vulcanization process consists of chemical reactions that create permanent covalent or ionic bonds, known as crosslinks, between adjacent molecules, which results in a complex interconnected network structure.<sup>1,42</sup> There are many factors that affect the degree of crosslinking including reactant concentration in the system, the mass of the

components in the system, and the time and temperature of the reaction. In theory, there would be a 1:1 ratio in molar reaction between the functional groups on each monomer. This would imply that a fully crosslinked plastic would have no residual reaction sites. In practice, the increasingly polymerized mass sequesters some reactive sites, creating side oligomers that are not a part of the larger reaction.<sup>43</sup> The mass of the crosslinking material can affect gelation. As the mass increases, the ability to transfer heat created at the reaction site is decreases. This is due to the thermally insulative nature of polymers and can lead to uncontrolled gelation or autoacceleration.<sup>43</sup>

Time and temperature also play a major part in crosslinking. As the molecular weight of the polymer increases, so does system viscosity. The material begins with low viscosity and increases with time. The viscosity increase will outpace any reduction from the heat generated by the reaction and continues until it reaches a gel point. From the gel point forward, the viscosity becomes infinite and the material is now a fully crosslinked thermoset material. Figure 8 shows the relationship between system viscosity and reaction time.<sup>43</sup>

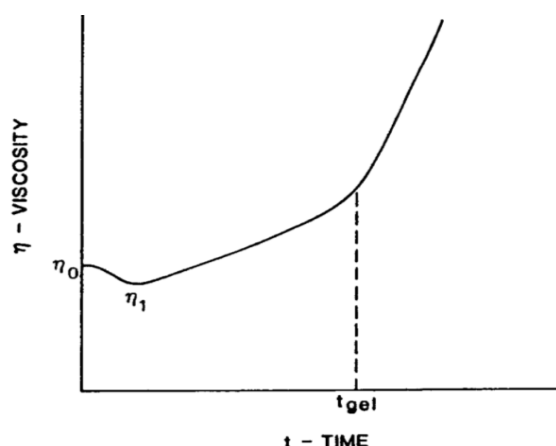


**Figure 7.** Graph representing crosslinking as a function of time and viscosity.<sup>43</sup>

Temperature has a similar effect as mass in crosslinking. The rate of viscosity increase depends on the temperature in system. Increasing crosslinking temperature



shortens the cure time while decreasing the temperature extends the curing time. Figure 9 demonstrates the effect of temperature on system viscosity.<sup>43</sup>

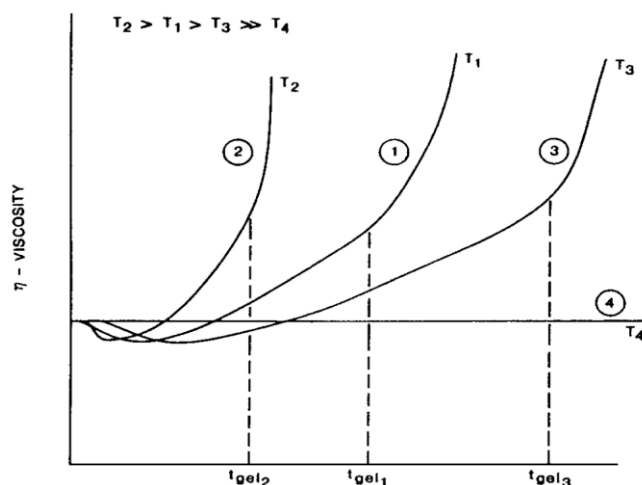


**Figure 8.** Viscosity vs. time at different curing temperatures: 1) standard temperature, 2) increased temperature, 3) decreased temperature, 4) temperature below reaction activation temperature.<sup>43</sup>

The activated cure method is one common approach for vulcanizing polysiloxane elastomers. Activated cure method uses a crosslinking agent, generally an organic peroxide, in conjunction with heat and pressure to accomplish vulcanization. The conditions under which vulcanization is performed, the degree of crosslinking, and the chemical nature of the crosslinks determine the mechanical properties of elastomers.<sup>1</sup> Most alkyl groups found on polysiloxanes, such as methyl, ethyl, and propyl, can be vulcanized with certain peroxides. If the polysiloxane contains vinyl groups, then vulcanization can occur and is affected by the concentration of those vinyl groups.<sup>44</sup>

The silicones industry heavily uses hydrosilylation reaction for vulcanization. Hydrosilylation uses highly active platinum catalysts, such as the silicone-soluble Karstedt's catalyst, with vinyl-silicon containing compounds, such as PDMS. Inhibitors to these catalysts help prevent premature crosslinking at ambient temperatures but permit

rapid crosslinking at higher temperatures. An example of hydrosilylation is given in Figure 9.<sup>45</sup>

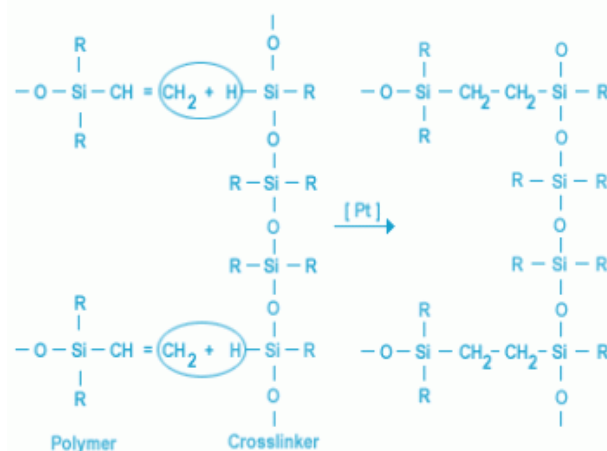


**Figure 9.** Hydrosilylation reaction with platinum catalysis.<sup>45</sup>

#### 1.4 Dynamic mechanical analysis

Elastomers rubbers are tested for different mechanical properties for industry use. These properties can range from shear strength to stiffness. The primary method used in this study to determine the mechanical properties of cured polysiloxanes is dynamic mechanical analysis (DMA). This characterization method allows different materials to be subjected to an oscillating force and characterizes the material response to that force.<sup>46</sup> Other factors that can affect this method are increasing or decreasing temperature, the length of the analysis, the frequency of force applied to the material, and how much force is used. Depending on the material to be analyzed, some specimens will need to be prepared to fit the dimensions of the apparatus, and this could include molding or cutting the specimen. Some of the different configurations used in DMA are compression, tension, bending, shearing, and cantilever configurations. Figure 10<sup>47</sup> shows the different stages for different analyses.

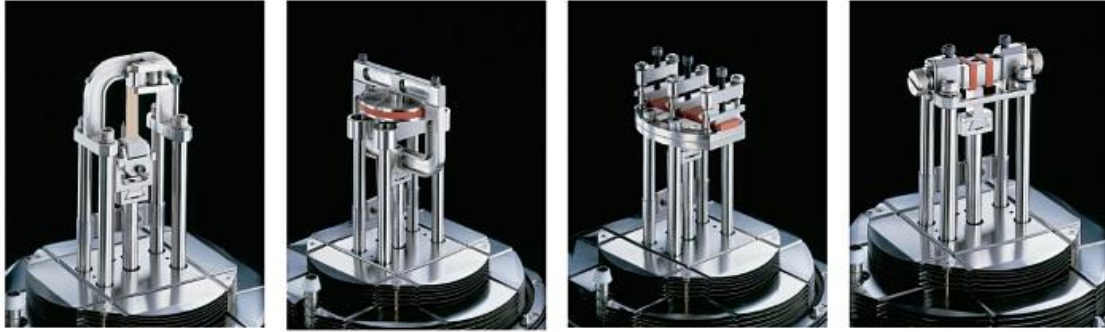


**Figure 10.** Examples of different DMA stages for different analytical techniques. Tension, compression, cantilever clamping for flexural analysis, and shear sandwich clamping (left to right).<sup>47</sup>

DMA uses an oscillating force applied to a material and measures the response to the force. The applied force is called stress and is designated sigma ( $\sigma$ ). The material that is subjected to the stress will show a deformation or strain, which is designated gamma ( $\gamma$ ). In a traditional stress/strain curve, the material will show a consistent strain curve as long the same force and temperature is applied. The slope of the line shows the relationship between stress and strain and measures the materials stiffness, or modulus. Figure 11 shows this relationship.<sup>46</sup> A major advantage of DMA is that the modulus can be recorded at each time the force is applied to the sample. If the measurement frequency is set to 1 Hertz (Hz) or 1 cycle/second, then the modulus would produce a value at every second of the test. The temperature and frequency can be increased and decreased over the duration of the test. This allow the mapping of the modulus as a function of temperature or frequency.

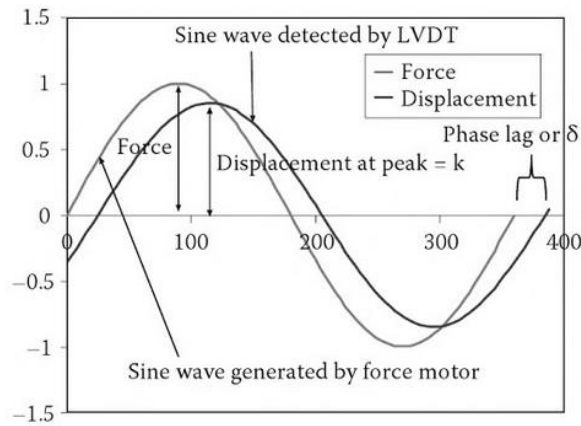


**Figure 11.** Typical stress/strain curve generated by DMA.<sup>46</sup>

The modulus measured by DMA is different than Young's modulus of a stress-strain curve. Young's modulus is taken from the initial linear slope of the stress-strain curve. The DMA complex modulus ( $E^*$ ) is taken from the elastic modulus ( $E'$ ) and the loss modulus ( $E''$ ) which is calculated from the materials response to the sine wave. This allows a better characterization of the material since the return energy ( $E'$ ) and the loss energy ( $E''$ ) of the material can be measured. The ratio of these effects ( $\tan \delta$ ) is called damping.<sup>46</sup>

Another important characterization that can be accomplished by DMA is creep-recovery. A constant low load, enough to stabilize the material, is added to a specimen. The test stress is then applied to the material, ideally instantly, and is held until the material reaches equilibrium. The material's responses are measured as a strain percent. A recovery test examines how the material relaxes when the stress is removed. The creep test can be used in two ways: 1) to gain basic information about a polymer or 2) to examine a polymer's response to certain test parameters. A linear equation can be used to calculate the equilibrium values for viscosity, modulus and compliance ( $J$ ). Compliance is defined as the willingness of a material to deform. This type of equation will not work for viscoelastic material, because polymers have a range of viscoelastic properties that

can be linear. The creep-recovery region of a polymer can be determined by performing a series of experiments on different specimen taken from the same sample and plot the results of creep compliance (J) over time. When the plots from each test of all the different specimen begin to overlay with each other, this is the linear viscoelastic region. One issue that can happen in a creep test, especially with viscoelastic material, is creep ringing. This can be addressed by changing experiment frequency or sample geometry.

Elastomers are ideal materials for DMA testing, especially highly crosslinked polymers. DMA is estimated to be 100 times more sensitive to measuring glass transitions than differential scanning calorimetry (DSC), and resolves other transitions, such as contributions of side chains of polymers, that DSC cannot detect.<sup>46,58</sup> There can be a 10 – 20 °C difference between the  $T_g$  as measured by DSC compared to the  $T_g$  measured by DMA. DMA can also display the effects of crosslinking in an elastomer as the reaction progresses. Because of the DMA's ability to measure different aspects of elastomers, DMA provides a more in-depth analysis of properties that result from crosslinking , such as molecular structure, composition, and environmental effects.<sup>46,49</sup>

## **CHAPTER II**

### **2. OBJECTIVES**

#### **2.1 Compounding polysiloxanes by twin-screw extrusion**

A model polysiloxane was compounded with a silica filler, two different crosslinkers, a catalyst and an inhibitor by twin-screw extrusion. The Process 11 was used to compound one commercially-available model polysiloxane with a synthetic, amorphous silica filler, two commercially-available model crosslinkers, one catalyst and one inhibitor to produce well-mixed silica-filled polysiloxane extrudate materials.

Prior to compounding, the silica filler, cross linker, catalysts and inhibitor were premixed into the polysiloxane in order to more conveniently feed the materials into the extruder. The premixed materials were then hand-fed into the Process 11 to be further processed into extrudate materials. The resulting compounded materials were expected to possess high thermal stability and, desirable rheological characteristics as well as superior mechanical properties once crosslinked.

The model copolymer was vinyl-terminated and its properties are listed as follows:

- PDV-0535 (CAS No: 68951-96-2)
  - Dimethyl-diphenylsiloxane copolymer
  - 4.0 - 6.0% diphenyl content
  - Molecular weight of 47,500 g/mol

The synthetic, amorphous silica filler is listed as follows:

- Hi-Sil™ 233-D (Hi-Sil-233D)
  - Synthetic reinforcing precipitated silica filler
  - Particle size: 64-77 $\mu$ m
  - Acquired from PPG Industries

The model crosslinkers were trimethylsiloxane-terminated and are listed as follows:

- HMS-082
  - Dimethyl-methylhdyrosiloxane
  - 7.0 - 9.0% methylhdyrosiloxane
  - Molecular weight of 5,500 g/mol
- HMS-151
  - Dimethyl-methylhdyrosiloxane
  - 15.0 - 18% methylhdyrosiloxane
  - Molecular weight of 2,000 g/mol

The Pt(acac)<sub>2</sub> catalyst was used as a solution in 1,3-dioxolane. The solution was agitated in a bottle and shielded from extraneous light to ensure longevity. The (MeCp)Pt(Me)<sub>3</sub> catalyst was used as a solution in 1,3-dioxolane. The solution was agitated in a bottle and shielded from extraneous light to ensure longevity. The inhibitor was used as a solution in toluene, agitated in a bottle and shielded from extraneous light. Either Pt(acac)<sub>2</sub> or (MeCp)Pt(Me)<sub>3</sub> catalyst was used in initial experiments to determine the catalyst type that would provide the longest shelf life.

Catalyst levels were varied as follows:

- Pt(acac)<sub>2</sub> 250 ppm
- Pt(acac)<sub>2</sub> 125 ppm

Inhibitor ratios were varied as follows:

- DEAD: Pt(acac)<sub>2</sub> 1:4
- DEAD: Pt(acac)<sub>2</sub> 1:2

## **2.2 Evaluation of filled model copolymer with different crosslinkers**

Crosslinker type, inhibitor ratio, and catalyst amount and type were evaluated and compared to determine the processing conditions necessary to obtain sufficient yield stress, degree of thixotropic behavior, advantageous mechanical properties, and appropriate shelf life. The composition, uniformity, and physical properties of filled polysiloxane materials were evaluated by thermogravimetric analysis (TGA), oscillatory rheometry, flow rheology, gel content, and dynamic mechanical analysis (DMA). The compounded materials were characterized for their yield stress, thixotropic behavior, viscoelastic behavior, and filler dispersion as determined by percent residue using TGA.

The model copolymer was compounded with two different crosslinkers, two different catalyst types, varied catalyst levels, and varied inhibitor ratios. The resulting compounded materials were evaluated by TGA, oscillatory rheometry, and flow rheology prior to UV-curing to determine shelf stability in dark conditions. The compounded materials were then UV-cured and evaluated for gel content and  $G'$  and  $\tan \delta$  as determined by DMA. The appropriate crosslinker, catalyst amount, catalyst-to-inhibitor ratio were determined to create a shelf-stable elastomeric material that had superior mechanical properties compared to commercial polysiloxane rubbers once fully UV-cured.



## **CHAPTER III**

### **3. EXPERIMENTAL**

#### **3.1 Materials**

##### **3.1.1 Commercial polysiloxane**

A commercially-available model polysiloxane was evaluated utilizing the Process 11 twin-screw extruder to determine the optimal formulation for polysiloxane materials. The commercially available polysiloxane was a vinyl-terminated (3.0 - 3.5% diphenylsiloxane)-dimethyl siloxane copolymer (model copolymer) PDV-0535 with a molecular weight of 27,000 g/mol. The commercially-available model polysiloxane was purchased from Gelest (Morrisville, Pennsylvania, United States of America).<sup>50</sup>

##### **3.1.2 Commercial filler**

One commercial synthetic amorphous silica filler was utilized for filling model polysiloxanes. Hi-Sil™ 233-D (Hi-Sil-233D) synthetic precipitated silica filler was purchased from PPG (College Station, Texas, United States of America)<sup>51</sup> with particle sizes ranging from 64 to 77  $\mu\text{m}$  and a surface area of 151  $\text{m}^2/\text{g}$ .

##### **3.1.3 Commercial crosslinkers**

Two crosslinkers were utilized in these experiments. The first commercially-available crosslinker (HMS-082) was a trimethylsiloxane terminated (7 - 9% methylhydrosiloxane)- dimethylsiloxane copolymer with a molecular weight of 5,500 -

6,500 g/mol. The second commercially-available crosslinker (HMS 151) was a trimethylsiloxane terminated (15 - 18% methylhydrosiloxane)-dimethylsiloxane copolymer with a molecular weight of 1,900 - 2,000 g/mol. Both crosslinkers were purchased from Gelest (Morrisville, Pennsylvania, United States).<sup>50</sup>

### **3.1.4 Catalysts and inhibitor**

Two catalysts and one inhibitor were utilized in these experiments. The catalysts were 2.4 wt% of the overall the system. The inhibitor was 1.4 wt% of the overall the system. The first catalyst was trimethyl(methylcyclopentadienyl)platinum(IV) ( $\text{MeCpPt}(\text{Me})_3$ ). The catalyst solution was created by adding 4.88 g of 1,3-dioxolane with 0.12 g of  $\text{MeCpPt}(\text{Me})_3$  in a glass vial. The vial is gently agitated to dissolve the catalyst. The vial was then wrapped in foil to prevent UV activation. The second catalyst was platinum (II) acetylacetonate ( $\text{Pt}(\text{acac})_2$ ). This catalyst was also created with the same procedure as the first catalyst, by dissolving 0.12 g of  $\text{Pt}(\text{acac})_2$  in 4.88g of 1,3-dioxolane. The inhibitor was diethyl azodicarboxylate (DEAD). The inhibitor solution was created by combining 4.335 g of toluene with 0.05 g of DEAD in a glass vial. The vial was then agitated and covered with foil.

## **3.2 Methods**

### **3.2.1 Polysiloxane materials processing**

The ThermoFisher Scientific Process 11 Parallel Twin-screw Extruder, Model 11 (Karlsruhe, Germany)<sup>52</sup> is a bench-top, lab-scale, twin-screw extruder. Figure 13 displays the Process 11 twin-screw extruder. The throughput rates can range from 20 g/hr to 2.5 kg/hr with realistic screw geometry and processing conditions that can be scalable for industrial compounding. The Process 11 contains a 40:1 L:D ratio barrel with two 11 mm

fully segmented, co-rotating screws. The Process 11 also contains a chiller unit that circulates water through the feed throat of the extruder to maintain a consistent feed throat temperature.<sup>53</sup>



**Figure 12.** Thermo Fisher Scientific Process 11 twin-screw extruder.<sup>53</sup>

This study utilizes the Process 11 twin-screw extruder to compound a commercially available model polysiloxane, two commercially available crosslinkers, catalysts, and inhibitor with silica filler. Prior to compounding, the polysiloxane, silica filler, crosslinkers, catalysts, and inhibitor were premixed for proper feeding into the extruder. The premixed material was then hand-fed into the Process 11 twin-screw extruder to be further mixed into extrudate material. The resulting silica-filled polysiloxane materials were expected to possess high thermal stability and desirable rheological characteristics prior to vulcanization and high mechanical properties after vulcanization because of the even distribution of the material. The polysiloxane compounded materials were characterized by thermogravimetric analysis (TGA), oscillatory rheometry, flow rheology, and dynamic mechanical analysis (DMA).

### **3.2.1.1 Premixing silica-filled polysiloxanes**

Prior to compounding, the silica filler was premixed with the polysiloxanes to prepare a paste-like material for proper feeding into the Process 11 twin-screw extruder. The polysiloxane, crosslinker, catalysis, and inhibitor were poured into a KitchenAid Classic 4.5 quart Mixer, Model K45SSWH (Benton Harbor, Michigan, United States of America),<sup>54</sup> and stirred for two minutes to allow each component to be thoroughly mixed. The filler was then added to the mixer at the desired loading level, and the formulations were mixed until a visually homogenous mixture was obtained.

### **3.2.1.2 Compounding silica-filled polysiloxanes**

The premixed commercially-available polysiloxanes with silica were compounded through the Process 11 twin-screw extruder. The parameters were set based on previous work<sup>17</sup>. The barrel and die temperature were set at 40°C. The chiller temperature (25 °C) was set relative to the temperature of the feed throat of the extruder. The screw speed (75 rpm) was set relative to the mixing ability of the Process 11 twin-screw extruder.

## **3.3 Characterization methods**

### **3.3.1 Thermal characterization by thermogravimetric analysis**

TGA was used to evaluate the distribution of filler in the silica-filled polysiloxane materials by using a TA Instruments Thermogravimetric Analyzer, Model 550 (New Castle, DE, United States).<sup>55</sup> An even distribution of filler was determined by observing the percent residue of three specimens per compounded extrudate material. All experiments were purged with nitrogen gas (60 mL/min purge flow rate), at a heating rate of 10°C/min to 700°C. The three specimens tested per extrudate material were taken from

the beginning of the compounding process, middle of the compounding process, and end of the compounding process. The temperature at 10% and 50% weight loss, as well as the residue percentage values of the compounded materials were recorded by TA Trios software.

### **3.3.2 Rheological characterization**

#### **3.3.2.1 Oscillatory rheometry**

Oscillatory rheometry was used to determine the rheological responses and yield stresses of the filled polysiloxane materials by using a TA Instruments Rotational Rheometer, Ltd AR2000EX (New Castle, DE, United States of America)<sup>55</sup> with a 40 mm diameter steel flat plate and a 1 mm gap at 25°C. The frequency was held constant at 1 Hertz and an oscillatory stress sweep from 3 Pa to 10,000 Pa was applied to the formulations. The results were obtained by TA Data Analysis software.

#### **3.3.2.2 Flow rheology**

The TA Instruments Rotational Rheometer AR2000EX was also used to perform flow rheology on the compounded materials. The rheometer used a 40 mm diameter steel flat plate and a 1 mm gap at 25°C. A linear shear rate from 0.01 sec<sup>-1</sup> to 10 sec<sup>-1</sup> was applied to the filled formulations, followed by a linear shear rate from 10 sec<sup>-1</sup> to 0.01 sec<sup>-1</sup>. The results were obtained by TA Data Analysis software.

### **3.3.3 Material curing**

#### **3.3.3.1 Dark curing for shelf stability determination**

The extrudate's shelf life was observed. Two pieces of uncured extrudate were placed into two different containers. One container was left on the countertop and was subjected to ambient light. The second container was placed inside a black container that

prevented any light permeation. Each sample was inspected daily until they crosslinked, and their properties recorded appropriately.

### **3.3.3.2 UV curing**

A sample from each polysiloxane extrudate was spread onto two rectangular aluminum molds, shown in Figure 13. The rectangular dimension was the same except that one was 0.5 mm deep while the other was 3 mm deep. The samples were then placed inside of an UVitron International SunRay 400 SM UV lamp (Springfield, MA, United States of America).<sup>56</sup> The samples were exposed to the lamp until the crosslinking reaction was complete. The samples were periodically inspected to monitor the vulcanization process. The time for each sample to complete the crosslinking reaction was recorded. The 3 mm film was used for further testing.



**Figure 13.** 3mm aluminum mold for UV curing of elastomers. 0.5mm mold is not shown.

### **3.3.4 Cured material analysis**

#### **3.3.4.1 Soxhlet extraction of vulcanized samples**

The gel content of the vulcanized materials was determined by Soxhlet extraction. Soxhlet extraction was used to determine the amount unreacted starting material is present in the crosslinked material. Specimens from the 0.5mm samples were cut, weighed, and placed inside a dried thimble. The thimble was then placed inside of an

extraction chamber. A condenser and boiling flask were placed above and below the chamber, respectively. The flask was filled with THF and heated to vapor, which then condensed to fill the thimble. After the thimble was filled with sufficient solvent, it begins to siphon back down to the flask. Figure 14 displays this extraction apparatus.<sup>57</sup>

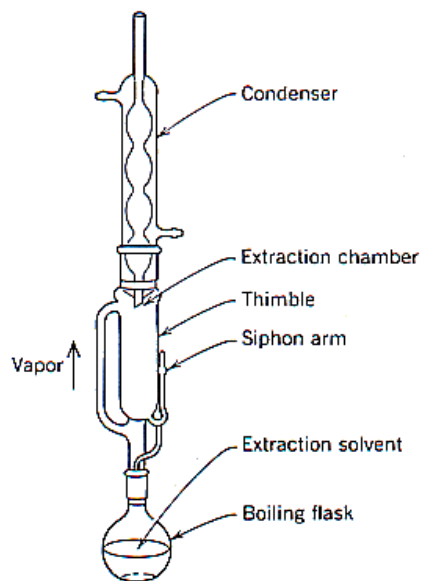


**Figure 14.** Soxhlet extraction apparatus.<sup>57</sup>

The Soxhlet extraction ran for three hours. The thimble was removed and dried to eliminate any excess moisture. The sample was removed from the thimble and weighed once more. The difference between the initial weight and final weight provided the gel content percentage.

#### **3.3.4.2 Dynamic mechanical analysis of vulcanized samples**

Dynamic mechanical analysis (DMA) was used to determine the mechanical properties of vulcanized materials as well as the  $T_g$ s. There are several different stages that can be used based on the orientation of the material. For this experiment, the shear sandwich stage was used. The shear sandwich stage is one of the most commonly used stages in DMA because of its ease of use and versatility with sample dimensions. For the purpose this experiment, the sandwich stage was used because it mimics a similar

mechanical response as the rheological studies performed. The thick film was cut into two 10 x 10mm squares and placed between the plates. Figure 15 shows the DMA shear sandwich stage.<sup>58</sup> The starting temperature was set to at -130 °C and was ramped up to 30 °C at a rate of 5 °C/min, with the frequency set to 1 Hz. The results were evaluated with the TA Universal Analysis software.



**Figure 15.** Dynamic mechanical analysis shear sandwich stage.<sup>58</sup>



## **CHAPTER IV**

### **4. RESULTS AND DISCUSSION**

#### **COMPARISON OF CATALYST TYPES IN FILLED SYSTEMS**

##### **4.1 Observations of commercial polysiloxane, filler, crosslinkers, catalyst, inhibitor, and compounded material.**

###### **4.1.1 Observations of commercial polysiloxane**

The commercial model copolymer was a transparent, colorless, viscous fluid. The appearance of the commercially-available polysiloxane is presented in Figure 16.

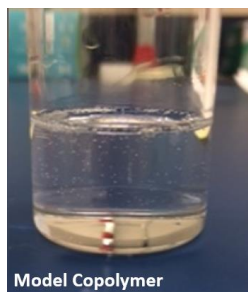


**Figure 16.** Appearance of the commercial polysiloxane PDV-0535.

###### **4.1.2 Observations of commercial filler**

The commercial filler was a white, flaky, powder. Figure 17 displays the appearance of the commercial synthetic amorphous silica filler.



**Figure 17.** Appearance of the commercial filler: Hi-Sil-233D.

#### 4.1.3 Observations of commercial crosslinkers

The commercial model crosslinkers were a transparent, colorless, viscous fluid.

Figure 18 displays the appearance of the commercial crosslinkers.

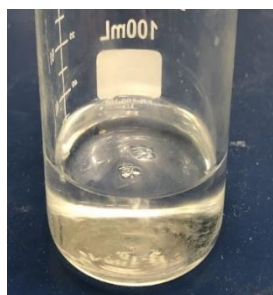


**Figure 18.** Appearance of the commercial crosslinker HMS-082. HMS-151 is not shown.

#### 4.1.4 Observations of catalysis and inhibitor

The catalysts and inhibitor were transparent, yellow-tinted, viscous fluids. All three had a slight odor. Figure 19 displays the appearance of the catalysts and inhibitors.

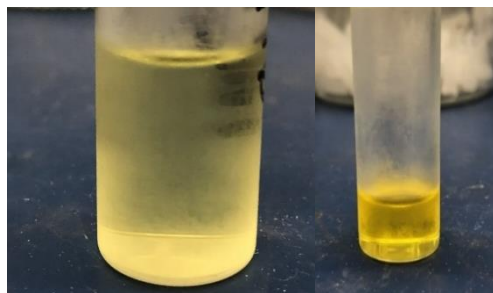


**Figure 19.** Appearance of the catalysts and inhibitor:  $\text{Pt}(\text{acac})_2$ , DEAD (left to right).  $(\text{MeCp})\text{Pt}(\text{Me})_3$  is not shown.

#### 4.1.5 Observations of filled compound material

The appearance of the filled model copolymer did not vary significantly between the different formulations. Figure 20 shows the appearance of the filled copolymer formulation.



**Figure 20.** Appearance of the filled model copolymer compounded material.

#### 4.2 Formulation of filled commercial polysiloxanes to compare catalyst types

The table below details the types and amounts of polysiloxane, fillers, crosslinkers, catalyst types, catalyst amounts, and inhibitor to catalyst ratios. In this chapter, the crosslinker types and catalyst types were varied and effects on thermal properties, rheological properties, and shelf stability were analyzed.

**Table 2.** Formulations details.

Polysiloxane	Filler	Crosslinker Type	Catalyst Type	[Catalyst] (ppm)	Inhibitor: Catalyst
PDV-0535	Hi-Sil-233D	HMS-082	(MeCp)Pt(Me) <sub>3</sub>	250	1:4
PDV-0535	Hi-Sil-233D	HMS-151	(MeCp)Pt(Me) <sub>3</sub>	250	1:4
PDV-0535	Hi-Sil-233D	HMS-082	Pt(acac) <sub>2</sub>	250	1:4
PDV-0535	Hi-Sil-233D	HMS-151	Pt(acac) <sub>2</sub>	250	1:4

#### 4.3 Thermogravimetric analysis of commercial polysiloxanes

Polysiloxanes contain incredibly high thermal stability that can be attributed to the partial-ionic character and high energy required to break the siloxane bond.<sup>59,60</sup>

Polysiloxanes generally degrade through heterolytic cleavage of the polysiloxane main chain, which releases volatile, low molecular weight products. The products are ultimately comprised of six- and eight-membered cyclic oligomeric compounds.<sup>59,61-63</sup>

Numerous literature studies have described one of the most common degradation schemes for PDMS to be intramolecular and back-biting depolymerization reactions of the siloxane backbone that results in the formation of the cyclic volatiles being released during decomposition.<sup>64-68</sup> The back-biting mechanism is similar to the secondary reactions that occur during the polysiloxane polymerization process and is shown in Figure 21.<sup>69</sup>

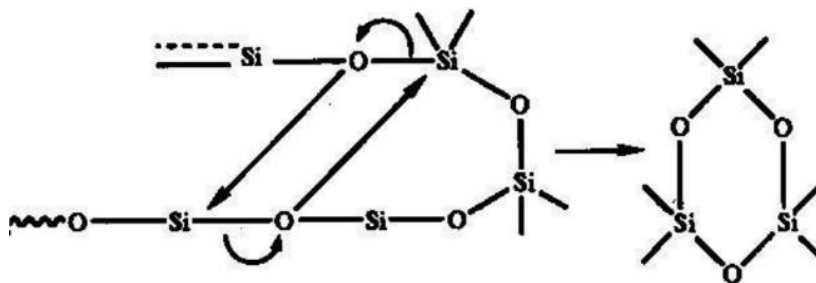


**Figure 21.** Back-biting depolymerization mechanism during thermal decomposition.<sup>69</sup>

Variations in solvents, end-group functionalities, and impurities can alter the degradation of PDMS.<sup>69</sup> However, the thermal stability of PDMS can be further enhanced with the incorporation of numerous functional groups, such as diphenyl-, diethyl-, and divinyl siloxy units to produce various copolymers.<sup>63,69,70</sup> These copolymers also back-bite to release volatile cyclic siloxanes during decomposition.<sup>70</sup>

#### 4.3.1 Thermogravimetric analysis of filled (MeCp)Pt(Me)<sub>3</sub> samples

The thermal stability and the filler dispersion of the PDV-0535-filled materials were investigated by TGA in a nitrogen atmosphere. The residue percentage values reported by TGA were examined to verify that the residue percentage was similar to the calculated filler loading amount. One specimen was assessed each day until the material crosslinked. This was to ensure that the filler was consistently dispersed at the desired calculated filler loading amount throughout the compounding process as well as to determine if there were any changes as crosslinking occurred.

Figure 22 displays the TGA thermograms of the filled PDV-0535 compounded with 28 wt% Hi-Sil-233D filler, HMS-082 crosslinker, (MeCp)Pt(Me)<sub>3</sub> catalyst and DEAD inhibitor. The curves in Figure 42 resemble typical TGA curves of silica-filled PDMS materials.<sup>22</sup> The temperature at 10% and 50% weight loss, as well as the residue percentage values of the filled compounded with 28 wt% Hi-Sil-233D filler are shown in Table 3. Table 3 shows the thermal properties versus time.

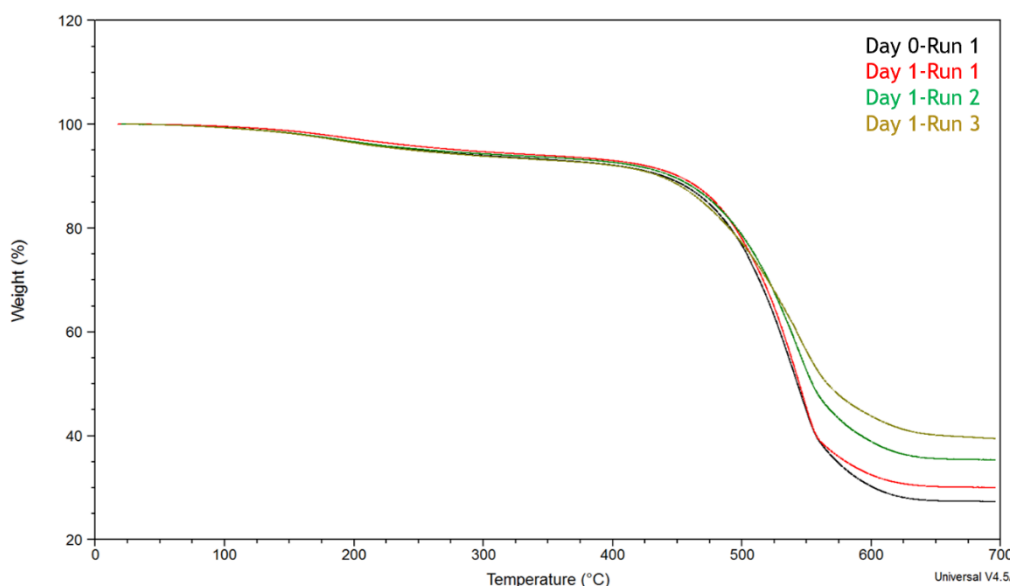


**Figure 22.** TGA thermograms of filled PDV-0535 compounded with 28 wt% Hi-Sil-233D filler, HMS-082 crosslinker, (MeCp)Pt(Me)<sub>3</sub> catalyst and DEAD inhibitor over time. Day 0 (—), Day 1 – Run 1 (—), Day 1 – Run 2 (—), Day 1 – Run 3 (—).

**Table 3.** Thermal properties of filled PDV-0535 compounded with 28 wt% Hi-Sil-233D filler, HMS-082 crosslinker, (MeCp)Pt(Me)<sub>3</sub> catalyst and DEAD inhibitor as crosslinking occurs.

Sample	Temperature at 10% Weight Loss (°C)	Temperature at 50% Weight Loss (°C)	Residue (%)
Day 0-Run 1	438	543	27.32
Day 1-Run 1	450	544	30.04
Day 1-Run 2	445	555	35.34
Day 1-Run 3	436	566	39.44

The filled materials possessed greater thermal stability compared to unfilled PDMS polymer.<sup>23,35-37,36-39,62,70</sup> The residue percentage values increased in value as the

crosslinking reaction continued, resulting in a residue that was 11 percent greater than the calculated filler amount.

It is commonly reported in literature that the incorporation of additives, such as fillers, can increase the thermal stability of polysiloxane materials.<sup>23,35-37,36-39,62,70</sup> The enhanced thermal stability of PDV-0535 compounded with Hi-Sil-233D filler could be attributed to the addition of the silica filler. Thermal stability in filled materials is attributed to the ability of the filler surface functional groups to interact with the polymer backbone through hydrogen bonding. Silica fillers have large surface areas with an abundance of silanol groups that interact with the polysiloxane backbone.<sup>14,15,18,23,37,62,71</sup> The polymer-filler interaction effects the polymer chains by hampering chain mobility. This results in an enhancement of thermal stability compared to unfilled polymers.<sup>20,38,72-74</sup>

Literature shows that while both (MeCp)Pt(Me)<sub>3</sub> and Pt(acac)<sub>2</sub> are UV-activated catalysts, they can also be activated by heat.<sup>75,76</sup> Steps were taken to try to minimize the amount of ambient UV light present during the compounding process in order to prevent premature crosslinking. However, it was discovered that during the TGA runs, the percent residue progressively increased. The residues increased as crosslinking occurred because of the heat activation in the catalysts.<sup>75,76</sup> Heat is caused during compounding by the friction that occurs in the mixing zones and against the barrel wall of the twin-screw extruder when silica is present within the formulation. This heat generation will initiate the crosslinking reaction.<sup>75,76,78</sup> As a result, the material was fully crosslinked one day after compounding. Additional filler can also further aggregate to create a stronger and

thicker protective silica barrier to hinder the release of the cyclic volatiles and enhance the thermal stability.<sup>26,77</sup>

Figure 23 displays the TGA thermograms of the filled PDV-0535 compounded with 28 wt% Hi-Sil-233D filler, HMS-151 crosslinker, (MeCp)Pt(Me)<sub>3</sub> catalyst and DEAD inhibitor. The temperature at 10% and 50% weight loss, as well as the residue percentage values of the filled compounded with 28 wt% Hi-Sil-233D filler are shown in Table 4. Table 4 shows the thermal properties versus time.

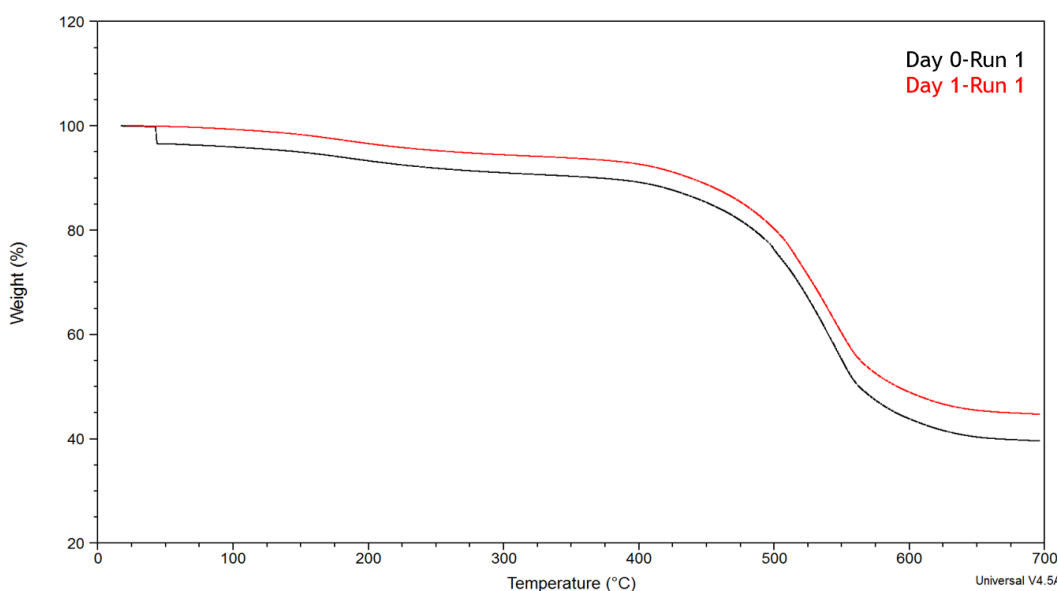


**Figure 23.** TGA thermograms of the filled PDV-0535 compounded with 28 wt% Hi-Sil-233D filler, HMS-151 crosslinker, (MeCp)Pt(Me)<sub>3</sub> catalyst and DEAD inhibitor over time. Day 0-Run 1 (—), Day 1-Run 1 (—).

**Table 4.** Thermal properties of the filled PDV-0535 compounded with 28 wt% Hi-Sil-233D filler, HMS-15 crosslinker, (MeCp)Pt(Me)<sub>3</sub> catalyst and DEAD inhibitor as crosslinking occurs.

Sample	Temperature at 10% Weight Loss (°C)	Temperature at 50% Weight Loss (°C)	Residue (%)
Day 0-Run 1	367	563	39.56
Day 1-Run 1	438	591	44.71

A similar increase in thermal stability and percent residue over time was observed due to the progression of crosslinking reaction initiated by heat generation during compounding. The material was fully crosslinked one day after compounding.

### 4.3.2 Thermogravimetric analysis of filled $\text{Pt}(\text{acac})_2$ samples

Figure 24 displays the TGA thermograms of the filled PDV-0535 compounded with 28 wt% Hi-Sil-233D filler, HMS-082 crosslinker,  $\text{Pt}(\text{acac})_2$  catalyst and DEAD inhibitor. The temperature at 10% and 50% weight loss, as well as the residue percentage values of the filled compounded with 28 wt% Hi-Sil-233D filler are shown in Table 5.

Table 5 shows the thermal properties versus time.

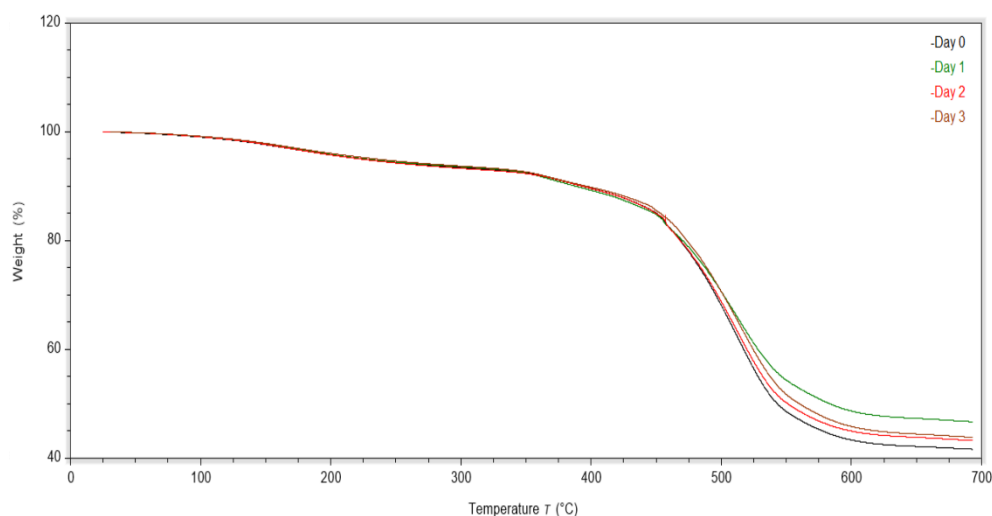


**Figure 24.** TGA thermograms of the filled PDV-0535 compounded with 28 wt% Hi-Sil-233D filler, HMS-082 crosslinker,  $\text{Pt}(\text{acac})_2$  catalyst and DEAD inhibitor over time. Day 0 (—), Day 1 (—), Day 2 (—), and Day 3 (—).

**Table 5.** Thermal properties of the filled PDV-0535 compounded with 28 wt% Hi-Sil-233D filler, HMS-082 crosslinker,  $\text{Pt}(\text{acac})_2$  catalyst and DEAD inhibitor as crosslinking occurs.

Sample	Temperature at 10% Weight Loss (°C)	Temperature at 50% Weight Loss (°C)	Residue (%)
Day 0	393	543	41.66
Day 1	388	583	46.72
Day 2	394	551	43.28
Day 3	396	560	43.88

There was no appreciable difference in thermal stability among the materials as the crosslinking reaction occurred. The residue percentage values were higher than the calculated filler amount. This is due to the heat activation of the catalyst.<sup>75,76,78,79</sup> Unlike



material formulated with (MeCp)Pt(Me)<sub>3</sub> catalyst, the material did not become fully crosslinked until three days after compounding. While the shelf stability was increased by the change in catalyst, the Pt(acac)<sub>2</sub> catalyst was still being activated by heat generated during compounding and the material crosslinked prematurely.

Figure 25 displays the TGA thermograms of the filled PDV-0535 compounded with 28 wt% Hi-Sil-233D filler, HMS-151 crosslinker, Pt(acac)<sub>2</sub> catalyst and DEAD inhibitor. The temperature at 10% and 50% weight loss, as well as the residue percentage values of the filled compounded with 28 wt% Hi-Sil-233D filler are shown in Table 6. Table 6 shows the thermal properties versus time.

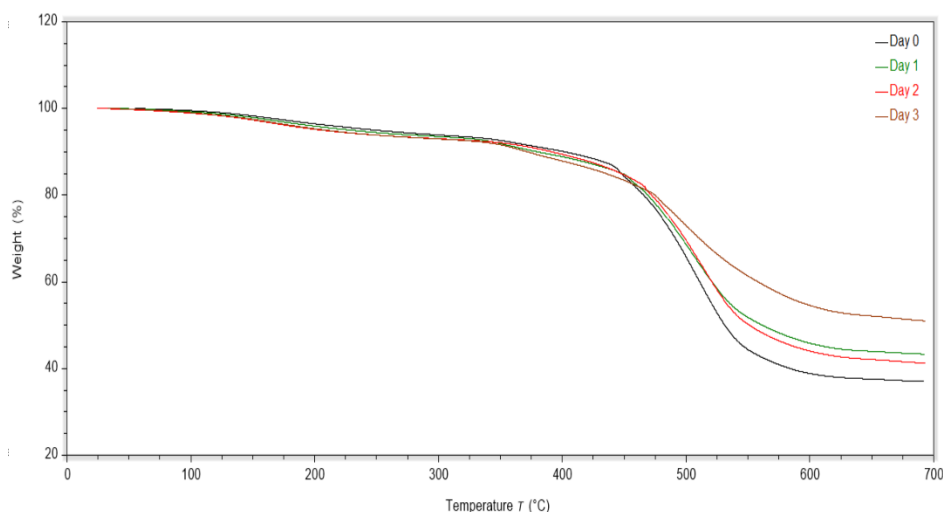


**Figure 25.** TGA thermograms of the filled PDV-0535 compounded with 28 wt% Hi-Sil-233D filler, HMS-151 crosslinker, Pt(acac)<sub>2</sub> catalyst and DEAD inhibitor as crosslinking occurs: Day 0 (—), Day 1 (—), Day 2 (—), and Day 3 (—).

**Table 6.** Thermal properties of the filled PDV-0535 compounded with 28 wt% Hi-Sil-233D filler, HMS-151 crosslinker, Pt(acac)<sub>2</sub> catalyst and DEAD inhibitor as crosslinking occurs.

Sample	Temperature at 10% Weight Loss (°C)	Temperature at 50% Weight Loss (°C)	Residue (%)
Day 0	401	531	37.02
Day 1	379	561	43.34
Day 2	388	551	41.26
Day 3	370	-	51.03

There was no appreciable difference in thermal stability among the samples. The residue percentage values were greater to the calculated filler loading amount. This is due to the heat activation of the catalyst.<sup>75-79</sup> The Pt(acac)<sub>2</sub> samples had longer cure time to compared to the (MeCp)Pt(Me)<sub>3</sub> samples. Marchi and company compared the reactivity between the two catalysts and determined that (MeCp)Pt(Me)<sub>3</sub> possessed a higher conversion rate and was more volatile with heat.<sup>75-79</sup>

#### 4.4 Oscillatory rheometry of filled commercial polysiloxanes

The yield stress of the commercial PDV-0535-filled materials was analyzed by oscillatory rheometry. The yield stress of the silica-filled materials was determined by the point at which the storage modulus ( $G'$ ) and loss modulus ( $G''$ ) curves intersect. Figure 26 shows this curve.<sup>17</sup>

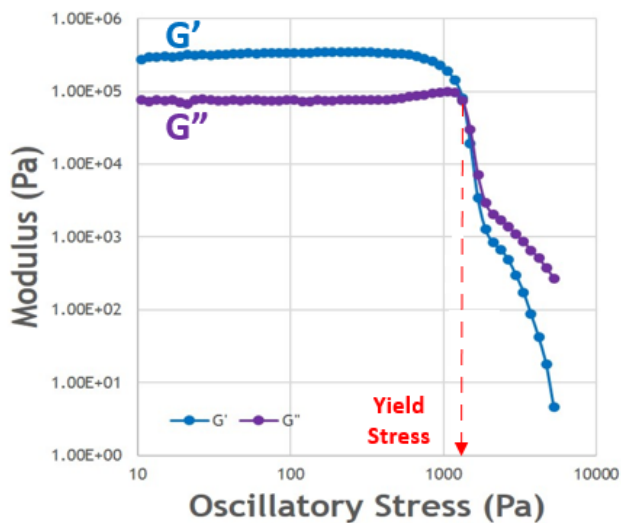


**Figure 26.** Storage and loss modulus versus oscillatory stress for a typical filled material. Yield stress is determined by the point where the  $G'$  (●) and  $G''$  (●) curves intersect.<sup>17</sup>

The aggregates are destroyed as the analysis continues by elevated shearing until the yield stress is obtained and the aggregated network structure is dismantled.<sup>30,32,80-83</sup> Thus,

an oscillatory stress sweep from 3 Pa to 5,000 Pa was applied to each of the samples one time per day, including the day the material was compounded, until it was crosslinked.

#### 4.4.1 Oscillatory rheometry of filled (MeCp)Pt(Me)<sub>3</sub> samples

Table 7 displays the yield stress values of the filled PDV-0535-Hi-Sil-233D-HMS-082-(MeCp)Pt(Me)<sub>3</sub>-DEAD taken each day.

**Table 7.** Yield stress of filled PDV-0535 compounded with 28 wt% Hi-Sil-233D filler, HMS-082 crosslinker, (MeCp)Pt(Me)<sub>3</sub> catalysis and DEAD inhibitor as crosslinking occurred over time.

Polysiloxane	Day	Yield Stress (Pa)
HMS-082-(MeCp)Pt(Me) <sub>3</sub> -DEAD	0	4,754
HMS-082-(MeCp)Pt(Me) <sub>3</sub> -DEAD	1	4,753

Only two days' worth of data could be collected as the material crosslinked on the third day. This is attributed to the volatile nature of the catalyst when subjected to UV and heat.<sup>75-79</sup>

Table 8 displays the yield stress values of the filled PDV-0535-Hi-Sil-233D-HMS-151-(MeCp)Pt(Me)<sub>3</sub>-DEAD as the taken each day. There was no data for Day 0 as the rheometer was experiencing technical difficulties.

**Table 8.** Yield stress of the filled PDV-0535 compounded with 28 wt% Hi-Sil-233D filler, HMS-151 crosslinker, (MeCp)Pt(Me)<sub>3</sub> catalysis and DEAD inhibitor as crosslinking occurs over time.

Polysiloxane	Day	Yield Stress (Pa)
HMS-151-(MeCp)Pt(Me) <sub>3</sub> -DEAD	1	1,685

Only one days' worth of data was collected because the material crosslinked on the second day.

#### 4.4.2 Oscillatory rheometry of filled Pt(acac)<sub>2</sub> samples

Table 9 displays the yield stress values of the filled PDV-0535-Hi-Sil-233D-HMS-082-Pt(acac)<sub>2</sub>-DEAD taken each day up to the point of curing.

**Table 9.** Yield stress of filled PDV-0535 compounded with 28 wt% Hi-Sil-233D filler, HMS-082 crosslinker, Pt(acac)<sub>2</sub> catalysis and DEAD inhibitor as crosslinking occurred over time.

Polysiloxane	Day	Yield Stress (Pa)
HMS-082-(Pt(acac) <sub>2</sub> )-DEAD	0	----
HMS-082-(Pt(acac) <sub>2</sub> )-DEAD	1	2,298
HMS-082-(Pt(acac) <sub>2</sub> )-DEAD	2	3,375
HMS-082-(Pt(acac) <sub>2</sub> )-DEAD	3	30

The day prior to full vulcanization had a yield stress that was significantly lower than both the previous data of the same material. This is due to a growing agglomerate network as curing proceeds. This will be discussed in greater detail in the next chapter.

Table 10 displays the yield stress values of the filled PDV-0535-Hi-Sil-233D-HMS-151-Pt(acac)<sub>2</sub>-DEAD as the taken each day up to the point of curing.

**Table 10.** Yield stress of filled PDV-0535 compounded with 28 wt% Hi-Sil-233D filler, HMS-151 crosslinker, Pt(acac)<sub>2</sub> catalysis and DEAD inhibitor as crosslinking occurred over time.

Polysiloxane	Day	Yield Stress (Pa)
HMS-151-(Pt(acac) <sub>2</sub> )-DEAD	0	2,123
HMS-151-(Pt(acac) <sub>2</sub> )-DEAD	1	4,247
HMS-151-(Pt(acac) <sub>2</sub> )-DEAD	2	3,774
HMS-151-(Pt(acac) <sub>2</sub> )-DEAD	3	1,339

The day prior to full vulcanization had a yield stress that was significantly lower than both the previous data of the same material similar to PDV-0535 compounded with 28 wt% Hi-Sil-233D filler, HMS-082 crosslinker, Pt(acac)<sub>2</sub> catalysis and DEAD inhibitor.

#### 4.5 Flow rheology of filled commercial polysiloxanes

The thixotropic behavior of the filled materials was characterized by studying the flow rheology of the filled polysiloxane systems. A sample from the materials was taken each day up to the point of curing. This was done by increasing a shear rate from 0.01 to

10  $\text{sec}^{-1}$  then decreasing from 10 to 0.01  $\text{sec}^{-1}$ . As the shear rate increased, the aggregated network of the polymer started to break down.<sup>17</sup> When the shear decreased, the network structure begins to relax and reform, as seen in Figure 27.<sup>17</sup>

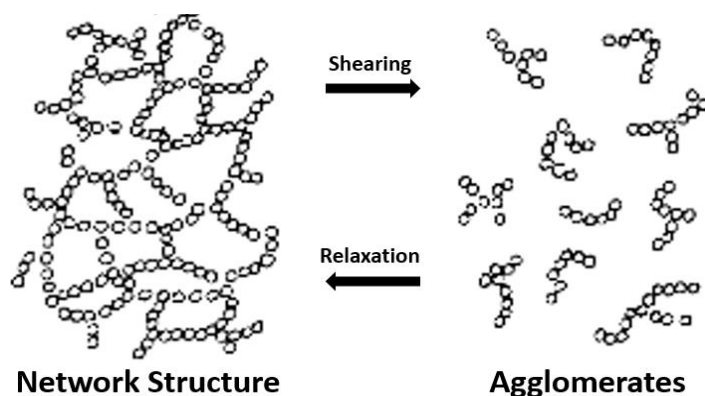


**Figure 27.** Deconstruction and reconstruction of polymer network.<sup>17</sup>

#### 4.5.1 Flow rheology of filled (MeCp)Pt(Me)<sub>3</sub> Samples

Figure 28 displays the thixotropic loops of the flow rheology analysis for the following filled commercial polysiloxane materials: PDV-0535 compounded with 28 wt% Hi-Sil-233D, (MeCp)Pt(Me)<sub>3</sub>, DEAD, and HMS-082 or HMS-151 over time as crosslinking occurred.

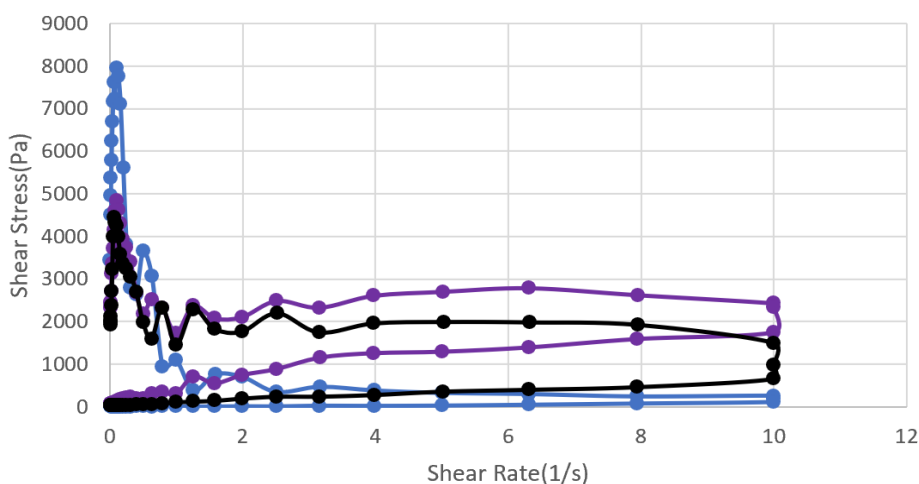


**Figure 28.** Thixotropic loops of flow rheology analysis filled PDV-0535 materials compounded with crosslinkers and (MeCp)Pt(Me):HMS-082 Day 0 (●), HMS-082 Day1 (●), and HMS-151 Day 1 (●).

The viscosity of the filled materials decreased as the shear rate increased, which was attributed to the destruction of the filler network structure by the increasing shear rates. The viscosity of the filled materials increased as the shear rate decreased, which was attributed to the reconstruction of the filler network. The HMS-082 on Day 0 has a more unstable viscosity compared to the other samples because of the relaxation of the polymer network.<sup>17</sup>

The HMS-082 Day 0 loop displays a shear-thinning behavior rather than a thixotropic behavior. The shear-thinning behavior is indicated by the thixotropic loops almost overlaying each other. This could be attributed to the permanent deformation of the network structure and inadequate time for the reconstruction of the network.<sup>84</sup> All other samples display thixotropic behavior.

#### 4.5.2 Flow rheology of filled $\text{Pt}(\text{acac})_2$ samples

Figure 29 displays the thixotropic loops of the flow rheology analysis for PDV-0535 compounded with 28 wt% Hi-Sil-233D,  $\text{Pt}(\text{acac})_2$ , DEAD, and HMS-082 over time as crosslinking occurred.

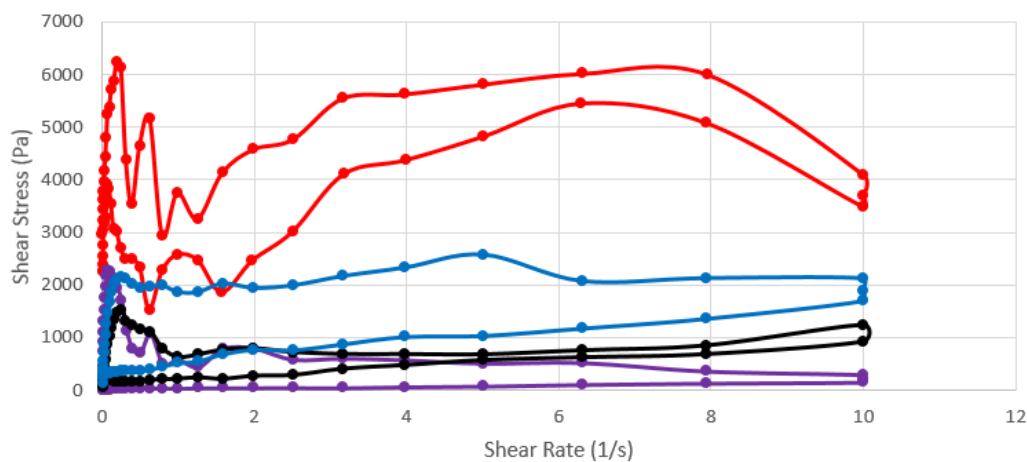


**Figure 29.** Thixotropic loops of flow rheology analysis filled material with HMS-082 and  $\text{Pt}(\text{acac})_2$ : Day 0 (●), Day 1 (●), Day 2 (●), and Day 3(●).

The viscosity of the filled materials decreased as the shear rate increased, which was attributed to the destruction of the filler network structure by the increasing shear rates. The viscosity of the filled materials increased as the shear rate decreased, which was attributed to the reconstruction of the filler network structure by the decreasing shear rates. The Day 0 sample has a greater viscosity compared to the other samples because of the relaxation of the polymer network after being compounded.<sup>17</sup>

The filled samples display thixotropic behavior but vary in the degree of thixotropy. A greater area within the thixotropic loop indicates a greater degree of thixotropy. The Day 0 data has an abnormal loop compared to Days 1 – 3 data. This was attributed to the relaxation of the polymer network immediately following compounding.<sup>17</sup> As the material crosslinked, a greater degree of thixotropy was observed over time, indicating an increase in thixotropy and greater time required for the aggregated networks to recover.

Figure 30 displays the thixotropic loops of the flow rheology analysis for PDV-0535 compounded with 28 wt% Hi-Sil-233D, Pt(acac)<sub>2</sub>, DEAD, and HMS-151 over time as crosslinking occurred.

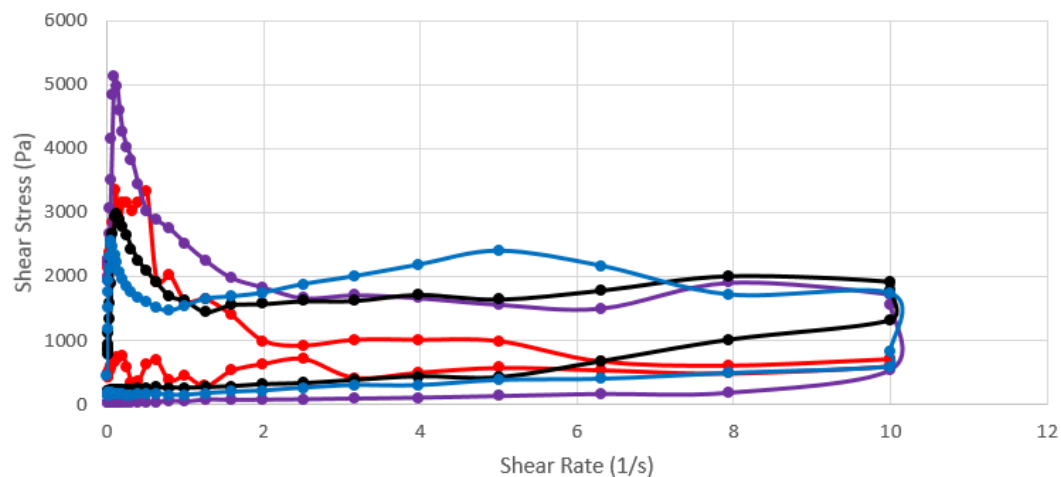


**Figure 30.** Thixotropic loops of flow rheology analysis for filled material with HMS-151 and  $\text{Pt}(\text{acac})_2$ : Day 0 (●), Day 1 (●), Day 2 (●), and Day 3(●).

The viscosity of the filled materials decreased as the shear rate increased, which was attributed to the destruction of the filler network structure by the increasing shear rates. The viscosity of the filled materials increased as the shear rate decreased, which was attributed to the reconstruction of the filler network structure by the decreasing shear rates. The Day 0 and Day 1 samples have a more volatile viscosity because of the relaxation of polymer.<sup>17</sup>

The filled sample displayed a thixotropic behavior. The Day 0 data has an abnormal loop compared to the other data. This is attributed to the relaxation of the polymer network immediately following compounding.<sup>17</sup> As the material crosslinked, a greater degree of thixotropy was observed over time compared to Day 0. In this case, however, as the material crosslinked, there was no significant change in degree of thixotropy as indicated by the area within the thixotropy loops. Days 1 – 3 all displayed a similar degree of thixotropy.



#### 4.6 Summary

The thermal stability, yield stress, and thixotropic behavior were greatly affected by the catalyst in the system. Since the catalysts were heat and UV activated, the materials begin crosslinking as they were compounded.  $(\text{MeCp})\text{Pt}(\text{Me})_3$  was more reactive to heat and UV compared to  $\text{Pt}(\text{acac})_2$ , causing those materials to crosslink in a shorter amount of time. The catalyst would also cause the crosslinking reaction to accelerate in the TGA, causing the residue to be higher than the calculated filler value. There was slight variation in the thixotropic behavior of the crosslinking material; the exception being the Day 0 of the  $\text{Pt}(\text{acac})_2$  and HMS-082. It is clear the  $(\text{MeCp})\text{Pt}(\text{Me})_3$  cures too quickly to be useful in an industry setting, as it shortens the shelf life beyond a reasonable limit.

## **CHAPTER V**

### **5. RESULTS AND DISCUSSION**

#### **COMPARISON OF CATALYST AND INHIBITOR LEVELS**

##### **5.1 Formulation modifications to extend shelf life**

Shelf stability studies indicated that  $(\text{MeCp})\text{Pt}(\text{Me})_3$  cured too rapidly once activated by heat during the compounding process to produce a commercially-viable formulation. For that reason,  $(\text{MeCp})\text{Pt}(\text{Me})_3$  was discontinued, and  $\text{Pt}(\text{acac})_2$  was developed further. Catalyst concentration and the ratio of inhibitor to catalyst was varied with the goal of extending and optimizing formulation shelf life.

The table below details the types and amounts of polysiloxane, fillers, crosslinkers, catalyst types, catalyst amounts, and inhibitor to catalyst ratios. In this chapter, the crosslinker types and catalyst types were varied and effects on thermal properties, rheological properties, and shelf stability were analyzed.

**Table 11.** Formulations details.

Polysiloxane	Filler	Crosslinker Type	Catalyst Type	[Catalyst] (ppm)	Inhibitor: Catalyst
PDV-0535	Hi-Sil-233D	HMS-151	Pt(acac) <sub>2</sub>	250	1:4
PDV-0535	Hi-Sil-233D	HMS-151	Pt(acac) <sub>2</sub>	250	1:2
PDV-0535	Hi-Sil-233D	HMS-151	Pt(acac) <sub>2</sub>	125	1:4
PDV-0535	Hi-Sil-233D	HMS-151	Pt(acac) <sub>2</sub>	125	1:2
PDV-0535	Hi-Sil-233D	HMS-082	Pt(acac) <sub>2</sub>	250	1:4
PDV-0535	Hi-Sil-233D	HMS-082	Pt(acac) <sub>2</sub>	250	1:2
PDV-0535	Hi-Sil-233D	HMS-082	Pt(acac) <sub>2</sub>	125	1:4
PDV-0535	Hi-Sil-233D	HMS-082	Pt(acac) <sub>2</sub>	125	1:2

## 5.2 Observations of filled model copolymer

The appearance of the filled model copolymer did not vary significantly between the different formulations. As with the previous experiment, the commercial polysiloxane is a transparent, colorless, viscous liquid. The commercial filler was a white flaky powder. Both commercial crosslinkers were transparent, colorless, viscous liquids. The catalyst and inhibitor were transparent, yellow-tinted, viscous fluids. Figure 31 shows the appearance of the filled copolymer formulation.



**Figure 31.** Appearance of the filled model copolymer compounded material.

## 5.3 Thermogravimetric analysis of filled model copolymer

The thermal stability and the filler dispersion of the filled model copolymer filled materials were investigated by TGA in a nitrogen atmosphere for the model copolymer-filled materials. One specimen was taken from the compounded extrudate material each day until the crosslinking reaction was completed. The residue percentage values were examined to verify an even distribution of filler by ensuring that the residue percentage

values were approximately equivalent to the calculated filler loading amount. As mentioned in the previous chapter, the catalyst used is reactive to UV and heat. This causes the residues in each experiment to be greater than the calculated filler amount.

Figure 32 displays the filled model copolymer compounded with 28 wt% Hi-Sil-233D filler, HMS-151 crosslinker, Pt(acac)<sub>2</sub> catalyst at a level of 250ppm, and DEAD inhibitor at a 1:4 ratio. The curves in Figure 53 resemble typical TGA curves of silica-filled polysiloxane materials.<sup>33,139,168</sup> The temperature at 10% and 50% weight loss, as well as the residue percentage values of the filled model copolymer compound are shown in Table 12. The values in Table 12 are taken from the sample each day until the crosslinking reaction is complete.

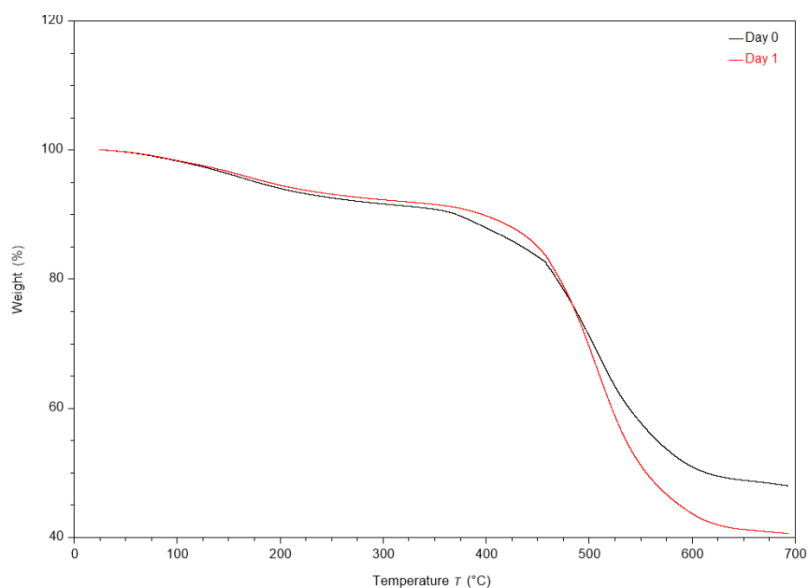


**Figure 32.** TGA thermograms of filled model copolymer compounded with HMS-151, Pt(acac)<sub>2</sub>(250ppm), and DEAD(1:4): Day 0 (—), and Day 1(—).

**Table 12.** Thermal properties of filled PDV-0535 compounded with 28 wt% Hi-Sil-233D filler, HMS-151 crosslinker, Pt(acac)<sub>2</sub> (250ppm) catalysis and DEAD (1:4) inhibitor as crosslinking occurred.

Polysiloxane	Temperature at 10% Weight Loss (°C)	Temperature at 50% Weight Loss (°C)	Residue (%)
Day 0	372	614	48.03
Day 1	396	556	40.65

The filled material had enhanced thermal stability compared to unfilled material.

The residue from each day are higher than the filler amount. This is due to the catalyst being reactive to heat, causing an oxidized charred crust around the specimens that reduced the rate of weight loss over the course of the TGA analysis.<sup>75-79</sup>

The enhanced thermal stability of the filled materials was attributed to the addition of the silica filler. The surface functional groups of the filler interact with the polymer backbone to create steric hindrance on the polymer chains and hamper their mobility.<sup>20,38,72-74</sup> The thermal stability enhancement of the filled materials was also attributed to the filler particles participating in aggregation.<sup>23</sup> Aggregates can interact with the polymer matrix to create a protective barrier that disrupts the release of cyclic volatiles during decomposition.<sup>22,25-27,62</sup>

Figure 33 displays the filled model copolymer compounded with 28 wt% Hi-Sil-233D filler, HMS-151 crosslinker, Pt(acac)<sub>2</sub> catalysts at a level of 250ppm, and DEAD inhibitor at a 1:2 ratio. The curves in Figure 54 resemble typical TGA curves of silica-filled polysiloxane materials.<sup>33,139,168</sup> The temperature at 10% and 50% weight loss, as well as the residue percentage values of the filled model copolymer compound are shown in Table 13. The values in Table 13 are taken from the sample each day until the crosslinking reaction was complete.

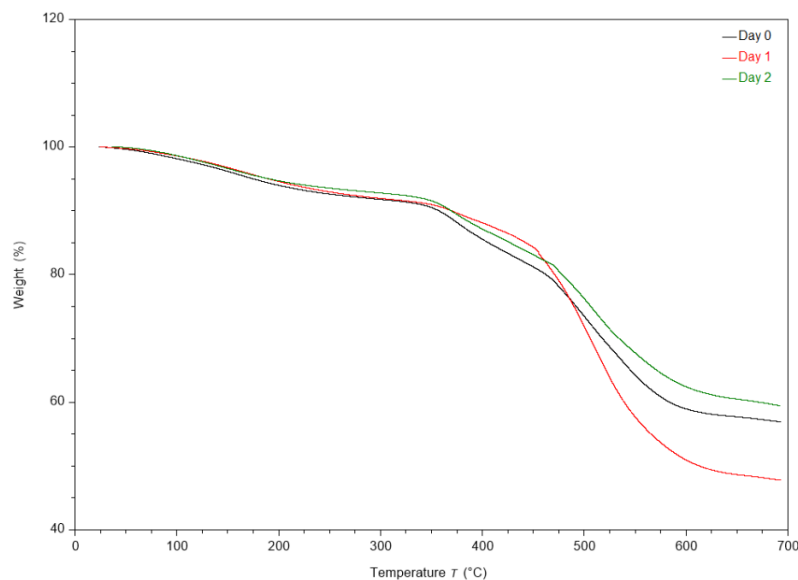


**Figure 33.** TGA thermograms of filled model copolymer compounded with HMS-151,  $\text{Pt}(\text{acac})_2$  (250ppm), and DEAD (1:2): Day 0 (—), Day 1 (—), and Day 2 (—).

**Table 13.** Thermal properties of filled PDV-0535 compounded with 28 wt% Hi-Sil-233D filler, HMS-151 crosslinker,  $\text{Pt}(\text{acac})_2$  (250ppm) catalysis and DEAD (1:2) inhibitor as crosslinking occurred.

Polysiloxane	Temperature at 10% Weight Loss (°C)	Temperature at 50% Weight Loss (°C)	Residue (%)
Day 0	357	-	56.93
Day 1	370	612	47.79
Day 2	369	-	59.48

Figure 34 displays the filled model copolymer compounded with 28 wt% Hi-Sil-233D filler, HMS-151 crosslinker,  $\text{Pt}(\text{acac})_2$  catalysts at a level of 125ppm, and DEAD inhibitor at a 1:4 ratio. The curves in Figure 55 resemble typical TGA curves of silica-filled polysiloxane materials.<sup>22,62</sup> The temperature at 10% and 50% weight loss, as well as the residue percentage values of the filled model copolymer compound are shown in Table 14. The values in Table 14 are taken from the sample each day until the crosslinking reaction was complete.

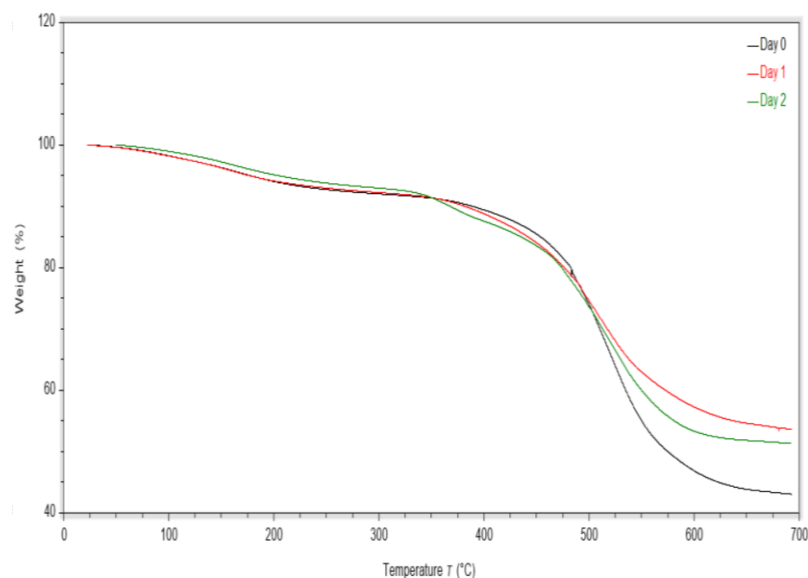


**Figure 34.** TGA thermograms of filled model copolymer compounded with HMS-151,  $\text{Pt}(\text{acac})_2$  (125ppm), and DEAD (1:4): Day 0 (—), Day 1 (—), and Day 2 (—).

**Table 14.** Thermal properties of filled PDV-0535 compounded with 28 wt% Hi-Sil-233D filler, HMS-151 crosslinker,  $\text{Pt}(\text{acac})_2$  (125ppm) catalysis and DEAD (1:4) inhibitor as crosslinking occurred.

Polysiloxane	Temperature at 10% Weight Loss (°C)	Temperature at 50% Weight Loss (°C)	Residue (%)
Day 0	389	575	43.08
Day 1	381	-	53.67
Day 2	368	-	51.35

Figure 35 displays the filled model copolymer compounded with 28 wt% Hi-Sil-233D filler, HMS-151 crosslinker,  $\text{Pt}(\text{acac})_2$  catalysts at a level of 125ppm, and DEAD inhibitor at a 1:2 ratio. The curves in Figure 56 resemble typical TGA curves of silica-filled polysiloxane materials.<sup>22,62</sup> The temperature at 10% and 50% weight loss, as well as the residue percentage values of the filled model copolymer compound are shown in Table 15. The values in Table 15 are taken from the sample each day until the crosslinking reaction was complete.

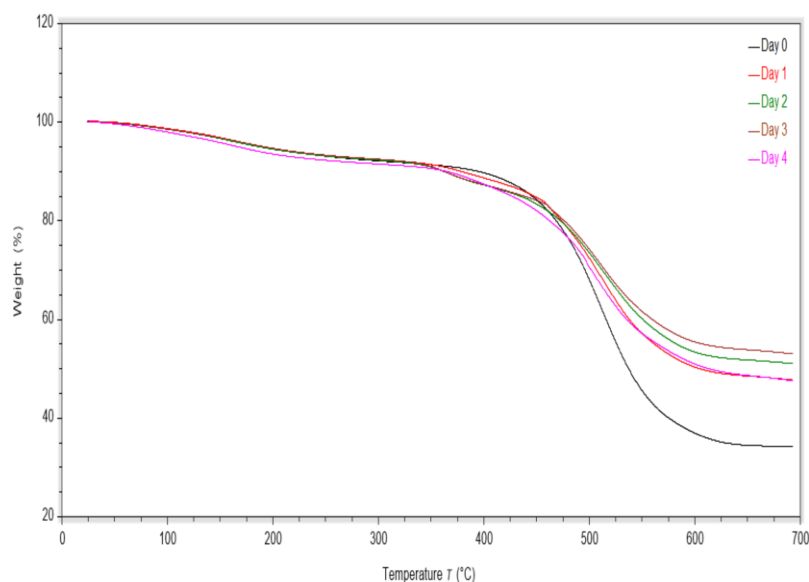


**Figure 35.** TGA thermograms of filled model copolymer compounded with HMS-151,  $\text{Pt}(\text{acac})_2$  (125ppm), and DEAD (1:2): Day 0 (—), Day 1 (—), Day 2 (—), Day 3 (—), and Day 4 (—).

**Table 15.** Thermal properties of filled PDV-0535 compounded with 28 wt% Hi-Sil-233D filler, HMS-151 crosslinker,  $\text{Pt}(\text{acac})_2$  (125ppm) catalysis and DEAD (1:2) inhibitor as crosslinking occurred.

Polysiloxane	Temperature at 10% Weight Loss (°C)	Temperature at 50% Weight Loss (°C)	Residue (%)
Day 0	380	-	53.68
Day 1	386	693	50.08
Day 2	357	560	43.84
Day 3	377	541	38.56
Day 4	366	614	47.64

Figure 36 displays the filled model copolymer compounded with 28 wt% Hi-Sil-233D filler, HMS-082 crosslinker,  $\text{Pt}(\text{acac})_2$  catalysts at a level of 250ppm, and DEAD inhibitor at a 1:4 ratio. The curves in Figure 57 resemble typical TGA curves of silica-filled polysiloxane materials.<sup>22,62</sup> The temperature at 10% and 50% weight loss, as well as the residue percentage values of the filled model copolymer compound are shown in Table 16. The values in Table 16 are taken from the sample each day until the crosslinking reaction was complete.



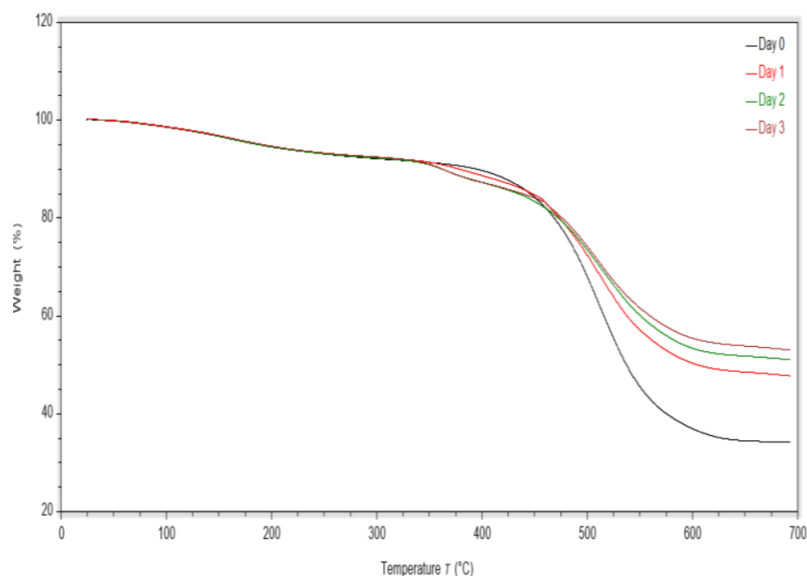


**Figure 36.** TGA thermograms of filled model copolymer compounded with HMS-082,  $\text{Pt}(\text{acac})_2$  (250ppm), and DEAD (1:4): Day 0 (—), Day 1 (—), Day 2 (—), and Day 3 (—).

**Table 16.** Thermal properties of filled PDV-0535 compounded with 28 wt% Hi-Sil-233D filler, HMS-082 crosslinker,  $\text{Pt}(\text{acac})_2$  (250ppm) catalysis and DEAD (1:4) inhibitor as crosslinking occurred.

Polysiloxane	Temperature at 10% Weight Loss (°C)	Temperature at 50% Weight Loss (°C)	Residue (%)
Day 0	396	537	34.16
Day 1	378	606	47.74
Day 2	362	-	51.09
Day 3	363	-	53.06

Figure 37 displays the filled model copolymer compounded with 28 wt% Hi-Sil-233D filler, HMS-082 crosslinker,  $\text{Pt}(\text{acac})_2$  catalysts at a level of 250ppm, and DEAD inhibitor at a 1:2 ratio. The curves in Figure 58 resemble typical TGA curves of silica-filled polysiloxane materials.<sup>22,62</sup> The temperature at 10% and 50% weight loss, as well as the residue percentage values of the filled model copolymer compound are shown in Table 17. The values in Table 17 are taken from the sample each day until the crosslinking reaction was complete.

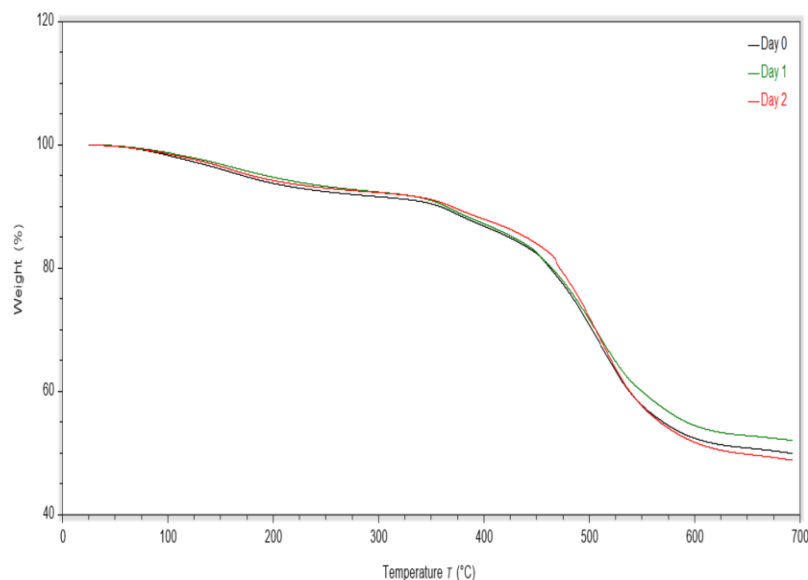


**Figure 37.** TGA thermograms of filled model copolymer compounded with HMS-082,  $\text{Pt}(\text{acac})_2$  (250ppm), and DEAD (1:2): Day 0 (—), Day 1 (—), and Day 2 (—).

**Table 17.** Thermal properties of filled PDV-0535 compounded with 28 wt% Hi-Sil-233D filler, HMS-082 crosslinker,  $\text{Pt}(\text{acac})_2$  (250ppm) catalysis and DEAD (1:2) inhibitor as crosslinking occurred.

Polysiloxane	Temperature at 10% Weight Loss (°C)	Temperature at 50% Weight Loss (°C)	Residue (%)
Day 0	359	693	50.04
Day 1	378	-	47.74
Day 2	369	640	48.92

Figure 38 displays the filled model copolymer compounded with 28 wt% Hi-Sil-233D filler, HMS-082 crosslinker,  $\text{Pt}(\text{acac})_2$  catalysts at a level of 125ppm, and DEAD inhibitor at a 1:4 ratio. The curves in Figure 59 resemble typical TGA curves of silica-filled polysiloxane materials.<sup>22,62</sup> The temperature at 10% and 50% weight loss, as well as the residue percentage values of the filled model copolymer compound are shown in Table 18. The values in Table 18 are taken from the sample each day until the crosslinking reaction was complete.

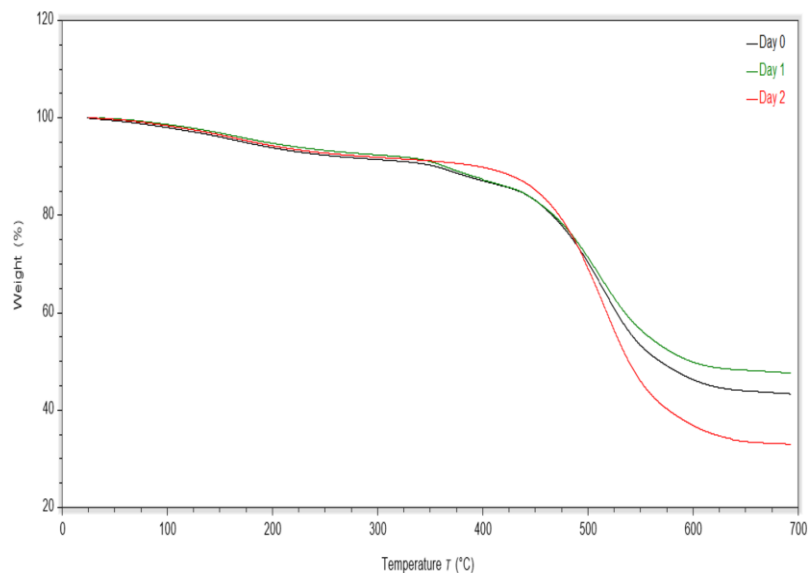


**Figure 38.** TGA thermograms of filled model copolymer compounded with HMS-082,  $\text{Pt}(\text{acac})_2$  (125ppm), and DEAD (1:4): Day 0 (—), Day 1 (—), and Day 2 (—).

**Table 18.** Thermal properties of filled PDV-0535 compounded with 28 wt% Hi-Sil-233D filler, HMS-082 crosslinker,  $\text{Pt}(\text{acac})_2$  (125ppm) catalysis and DEAD (1:4) inhibitor as crosslinking occurred.

Polysiloxane	Temperature at 10% Weight Loss (°C)	Temperature at 50% Weight Loss (°C)	Residue (%)
Day 0	355	568	43.35
Day 1	364	597	47.62
Day 2	398	539	33.02

Figure 39 displays the filled model copolymer compounded with 28 wt% Hi-Sil-233D filler, HMS-082 crosslinker,  $\text{Pt}(\text{acac})_2$  catalysts at a level of 125ppm, and DEAD inhibitor at a 1:2 ratio. The curves in Figure 60 resemble typical TGA curves of silica-filled polysiloxane materials.<sup>22,62</sup> The temperature at 10% and 50% weight loss, as well as the residue percentage values of the filled model copolymer compound are shown in Table 19. The values in Table 19 are taken from the sample each day until the crosslinking reaction was complete.

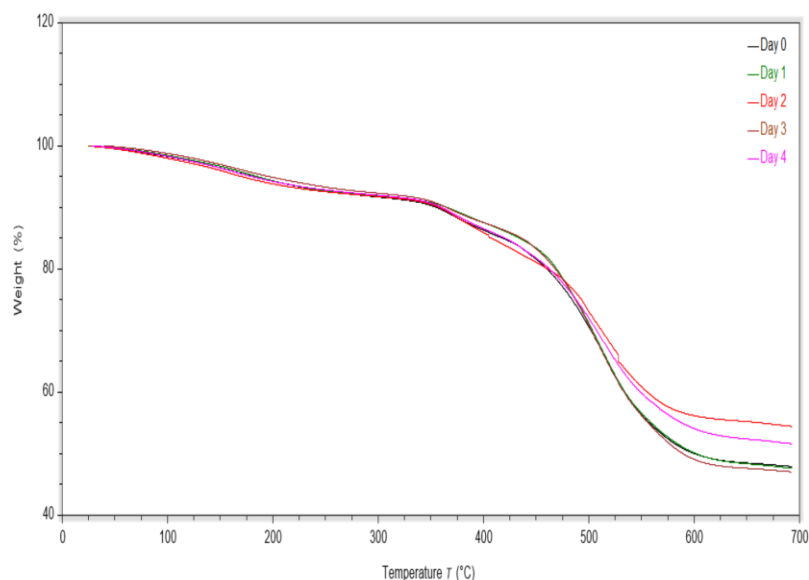


**Figure 39.** TGA thermograms of the filled model copolymer compounded with HMS-082,  $\text{Pt}(\text{acac})_2$  (125ppm), and DEAD (1:2): Day 0 (—), Day 1 (—), Day 2 (—), Day 3 (—), and Day 4 (—).

**Table 19.** Thermal properties of the filled PDV-0535 compounded with 28 wt% Hi-Sil-233D filler, HMS-082 crosslinker,  $\text{Pt}(\text{acac})_2$  (125ppm) catalysis and DEAD (1:2) inhibitor as crosslinking occurred.

Polysiloxane	Temperature at 10% Weight Loss (°C)	Temperature at 50% Weight Loss (°C)	Residue (%)
Day 0	356	600	47.96
Day 1	366	602	47.66
Day 2	358	-	54.46
Day 3	365	589	47.09
Day 4	350	-	51.67

The residue percentage values were greater to the calculated filler loading amount. This is due to the heat activation of the catalyst.<sup>75-79</sup> The formulations that contained  $\text{Pt}(\text{acac})_2$  at 125ppm and an inhibitor ratio of 1:2 had the longest shelf stability compared to other formulations because of the smaller amount of catalyst.<sup>75-79</sup>

#### 5.4 Oscillatory rheometry of filled commercial copolymer

The yield stress of the commercial PDV-0535-filled materials were analyzed by oscillatory rheometry. The yield stress of the silica-filled material was determined by the point at which the storage modulus and loss modulus curves intersect. Thus, an oscillatory stress sweep from 3 Pa to 10,000 Pa was applied to each of the samples one

time per day, including the day the material was compounded, until it was crosslinked.

Table 20 displays the yield stress values of the filled samples with HMS-151 crosslinker, Pt(acac)<sub>2</sub> (250ppm), and DEAD (1:4) taken each day.

**Table 20.** Yield stress of filled model copolymer compounded with HMS-151, Pt(acac)<sub>2</sub> (250ppm) and DEAD (1:4) each day until crosslinked.

Polysiloxane	Day	Yield Stress (Pa)
HMS-151-250ppm-1:4	0	9,487
HMS-151-250ppm-1:4	1	5,984

The yield stress values for the filled model copolymer compounded with HMS-151, Pt(acac)<sub>2</sub> (250ppm), and DEAD (1:2) compared each day to the reference silicone are shown in Table 21.

**Table 21.** Yield stress of filled model copolymer compounded with HMS-151, Pt(acac)<sub>2</sub> (250ppm) and DEAD (1:2) each day until crosslinked.

Polysiloxane	Day	Yield Stress (Pa)
HMS-151-250ppm- 1:2	0	7,535
HMS-151-250ppm- 1:2	1	3,774
HMS-151-250ppm- 1:2	2	1,890

The day zero values are unusual because of how the polymer system is configuring and relaxing after twin-screw extrusion. The last day before crosslinking had a dramatically lower level than the previous day. This can be explained by two different phenomena. The first reason is due to the gap between the screws. Before extensive processing with silica, the screws were fully intermeshed. They have become worn down from consistent use of the silica filler over time, which has caused the screws to degrade. While this gap is not massive, more particles remain agglomerated and are not broken down by the kneading zones. This leads to the second issue: the interaction between these agglomerates with the aggregated network. Giuseppe and company investigated the rheological properties of silica colloids. They noted that as the particle size of the silica

increased, the material started to show diminishing elastic properties. This is due to the growing agglomerate network subjected to stress, pushing the particles closer together and decreasing the yield stress as agglomeration increased.<sup>85</sup>

Table 22 displays the yield stress values for the filled model copolymer compounded with HMS-151, Pt(acac)<sub>2</sub> (125ppm), and DEAD (1:4) compared each day.

**Table 22.** Yield stress of filled model copolymer compounded with HMS-151, Pt(acac)<sub>2</sub> (125ppm) and DEAD (1:4) each day until crosslinked.

Polysiloxane	Day	Yield Stress (Pa)
HMS-151-125ppm-1:4	0	5,985
HMS-151-125ppm-1:4	1	3,775
HMS-151-125ppm-1:4	2	1,890

The decreasing yield stress as crosslinking occurs is due to the agglomerates in the system being pushed together, causing diminished elastic properties.<sup>85</sup> This leads to a decrease in yield stress before curing is complete and network is set in place.

Table 23 displays the yield stress values for the filled model copolymer compounded with HMS-151, Pt(acac)<sub>2</sub> (125ppm), and DEAD (1:2) compared each day.

**Table 23.** Yield stress of filled model copolymer compounded with HMS-151, Pt(acac)<sub>2</sub> (125ppm) and DEAD (1:2) each day until crosslinked.

Polysiloxane	Day	Yield Stress (Pa)
HMS-151-125ppm-1:2	0	1,503
HMS-151-125ppm-1:2	1	4,754
HMS-151-125ppm-1:2	2	2,998
HMS-151-125ppm-1:2	3	1,502
HMS-151-125ppm-1:2	4	377

The decreasing yield stress as crosslinking occurs is due to the agglomerates in the system being pushed together, causing diminished elastic properties.<sup>85</sup> This leads to a decrease in yield stress before curing is complete and the network is set in place.

Table 24 displays the yield stress values for the filled model copolymer compounded with HMS-082, Pt(acac)<sub>2</sub> (250ppm), and DEAD (1:4) compared each day.

**Table 24.** Yield stress of filled model copolymer compounded with HMS-082, Pt(acac)<sub>2</sub> (250ppm) and DEAD (1:4) each day until crosslinked.

Polysiloxane	Day	Yield Stress (Pa)
HMS-082-250ppm-1:4	0	1,503
HMS-082-250ppm-1:4	1	4,754
HMS-082-250ppm-1:4	2	2,998
HMS-082-250ppm-1:4	3	1,502

The yield stress is lower on the day of compounding and the day before it crosslinks. The yield stress on the day of compounding can be contributed to the system reorganizing itself after being extruded. The decreasing yield stress is contributed to the growing agglomerates in the material as crosslinking occurs.<sup>85</sup> This leads to a decrease in yield stress before curing is complete and the network is set in place.

Table 25 displays the yield stress values for the filled model copolymer compounded with HMS-082, Pt(acac)<sub>2</sub> (250ppm), and DEAD (1:2) compared each day to the reference silicone.

**Table 25.** Yield stress of filled model copolymer compounded with HMS-082, Pt(acac)<sub>2</sub> (250ppm) and DEAD (1:2) each day until crosslinked.

Polysiloxane	Day	Yield Stress (Pa)
HMS-082-250ppm-1:4	0	3,776
HMS-082-250ppm-1:4	1	1,192
HMS-082-250ppm-1:4	2	753

The decreasing yield stress as crosslinking occurs is due to the agglomerates in the system being pushed together, causing diminished elastic properties.<sup>85</sup> This leads to a decrease in yield stress before curing is complete and network is set in place.

Table 26 displays the yield stress values for the filled model copolymer compounded with HMS-082, Pt(acac)<sub>2</sub> (125ppm), and DEAD (1:4) compared each day.

**Table 26.** Yield stress of filled model copolymer compounded with HMS-082, Pt(acac)<sub>2</sub> (125ppm) and DEAD (1:4) each day until crosslinked.

Polysiloxane	Day	Yield Stress (Pa)
HMS-082-125ppm-1:4	0	7,535
HMS-082-125ppm-1:4	1	3,776
HMS-082-125ppm-1:4	2	1,384

The decreasing yield stress as crosslinking occurs is due to the agglomerates in the system being pushed together, causing diminished elastic properties.<sup>85</sup> This leads to a decrease in yield stress before curing is complete and network is set in place.

Table 27 displays the yield stress values for the filled model copolymer compounded with HMS-082, Pt(acac)<sub>2</sub> (125ppm), and DEAD (1:2) compared each day to the reference silicone.

**Table 27.** Yield stress of the filled model copolymer compounded with HMS-082, Pt(acac)<sub>2</sub> (125ppm) and DEAD (1:2) each day until crosslinked.

Polysiloxane	Day	Yield Stress (Pa)
HMS-082-125ppm-1:2	0	5,985
HMS-082-125ppm-1:2	1	2,999
HMS-082-125ppm-1:2	2	3,774
HMS-082-125ppm-1:2	3	1,891
HMS-082-125ppm-1:2	4	765

The decreasing yield stress as crosslinking occurs is due to the agglomerates in the system being pushed together, causing diminished elastic properties.<sup>85</sup> This leads to a decrease in yield stress before curing is complete and network is set in place.

## 5.5 Flow rheology of filled model copolymer

The thixotropic behavior of the model copolymer-filled materials was characterized by studying the flow rheology of the filled polysiloxane systems. A sample from each formulation was taken each day.



Figure 40 displays the thixotropic loops of the flow rheology analysis for filled PDV-0535-Hi-Sil-233D-HMS-151-Pt(acac)<sub>2</sub> (250ppm)- DEAD (1:4). The polymer network has started to crosslink because of the heat and pressure from the extruder; this coupled with the deconstruction and reconstruction of the network causes the irregular shape of the loops.

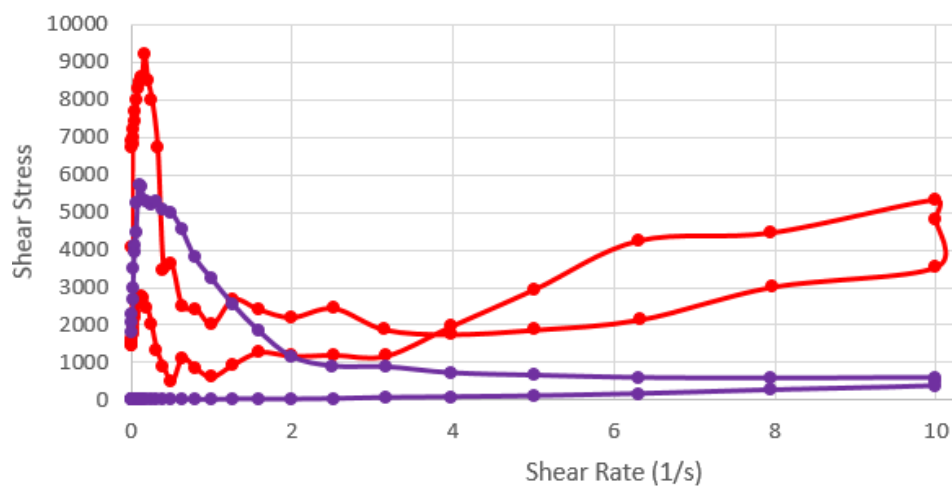


**Figure 40.** Thixotropic loops of the flow rheology for the reference silicone compared to the filled model copolymer materials compounded with HMS-151, Pt(acac)<sub>2</sub> (250ppm), and DEAD (1:4): Day 0 (●), and Day 1 (●).

The viscosity of the filled materials decreased as the shear rate increased, which was attributed to the destruction of the filler network structure by the increasing shear rates.<sup>86,87</sup> The day zero viscosity is high because of the reorganization of the network system. The viscosity of the filled materials increased as the shear rate decreased, which was again attributed to the reconstruction of the filler network structure over time.<sup>84</sup> The day one viscosity is low because of the bulk size of the particles.<sup>88</sup> The degree of thixotropy was not greatly affected by the curing process.

Figure 41 displays the thixotropic loops of the flow rheology analysis for filled PDV-0535-Hi-Sil-233D-HMS-151-Pt(acac)<sub>2</sub> (250ppm)-DEAD (1:2).

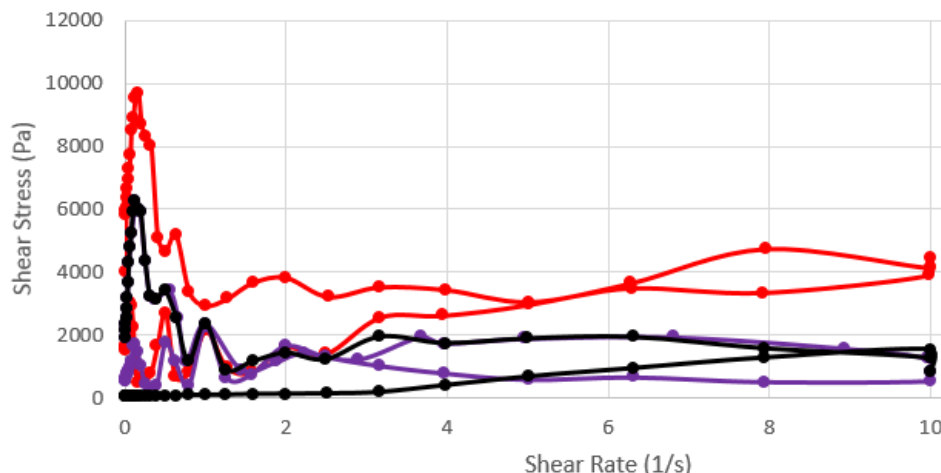


**Figure 41.** Thixotropic loops of the flow rheology for the reference silicone compared to the filled model copolymer materials compounded with HMS-151, Pt(acac)<sub>2</sub> (250ppm), and DEAD (1:2): Day 0 (●), Day 1 (●), and Day 2 (●).

The rheological behavior was similar to that of PDV-0535-Hi-Sil-233D-HMS-151-Pt(acac)<sub>2</sub> (250ppm)- DEAD (1:4).

Figure 42 displays the thixotropic loops of the flow rheology analysis for filled PDV-0535-Hi-Sil-233D-HMS-151-Pt(acac)<sub>2</sub> (125ppm)- DEAD (1:4).

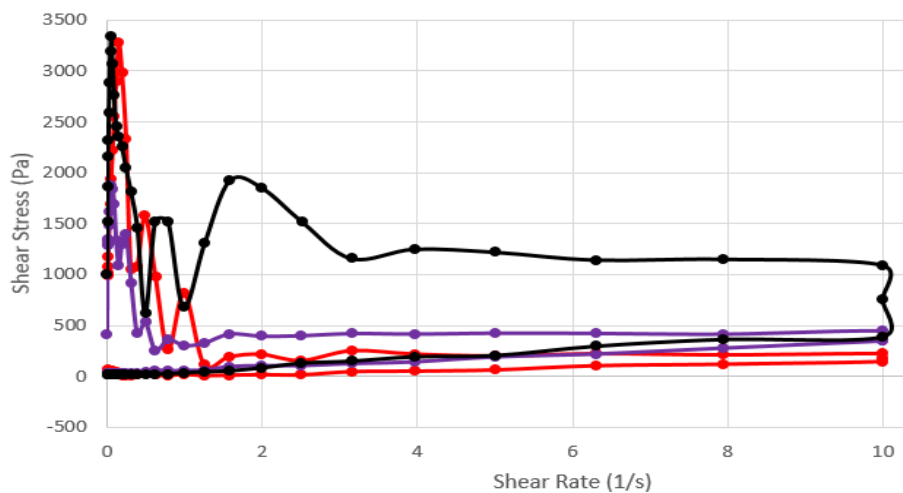


**Figure 42.** Thixotropic loops of the flow rheology analysis for the reference silicone compared to the filled model copolymer materials compounded with HMS-151, Pt(acac)<sub>2</sub> (125ppm), and DEAD (1:4): Day 0 (●), Day 1 (●), and Day 2 (●).

The rheological behavior was similar to PDV-0535-Hi-Sil-233D-HMS-151-Pt(acac)<sub>2</sub>- DEAD at 250 ppm catalyst concentration.

Figure 43 displays the thixotropic loops of the flow rheology analysis for filled PDV-0535-Hi-Sil-233D-HMS-151-Pt(acac)<sub>2</sub> (125ppm)- DEAD (1:2).

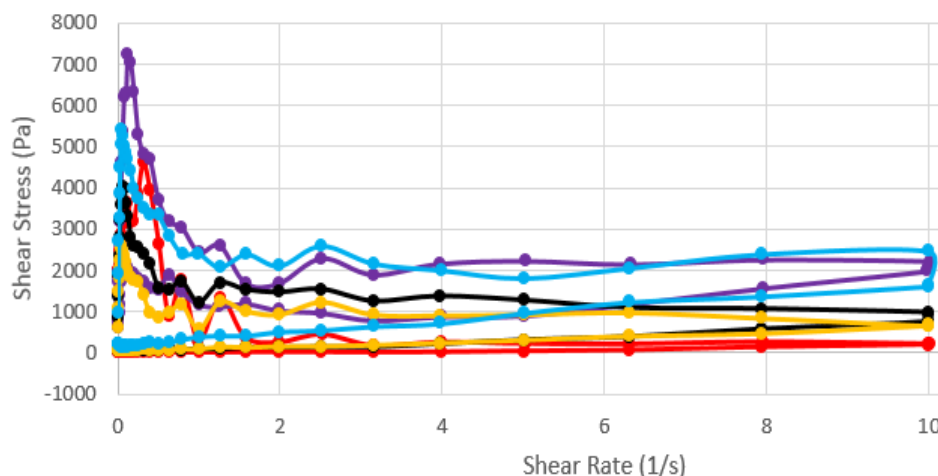


**Figure 43.** Thixotropic loops of the flow rheology analysis for the reference silicone compared to the filled model copolymer materials compounded with HMS-151, Pt(acac)<sub>2</sub> (125ppm), and DEAD (1:2): Day 0 (●), Day 1 (●), Day 2 (●), Day 3 (●), and Day 4 (●).

The rheological behavior was similar to PDV-0535-Hi-Sil-233D-HMS-151-Pt(acac)<sub>2</sub>-DEAD samples at 250 ppm catalyst concentration and PDV-0535-Hi-Sil-233D-HMS-151-Pt(acac)<sub>2</sub> (125ppm)- DEAD (1:4).

Figure 44 displays the thixotropic loops of the flow rheology analysis for filled PDV-0535-Hi-Sil-233D-HMS-082-Pt(acac)<sub>2</sub> (250ppm)- DEAD (1:4). The polymer network has started to crosslink because of the heat and pressure from the extruder; this coupled with the deconstruction and reconstruction of the network causes the irregular shape of the loops.

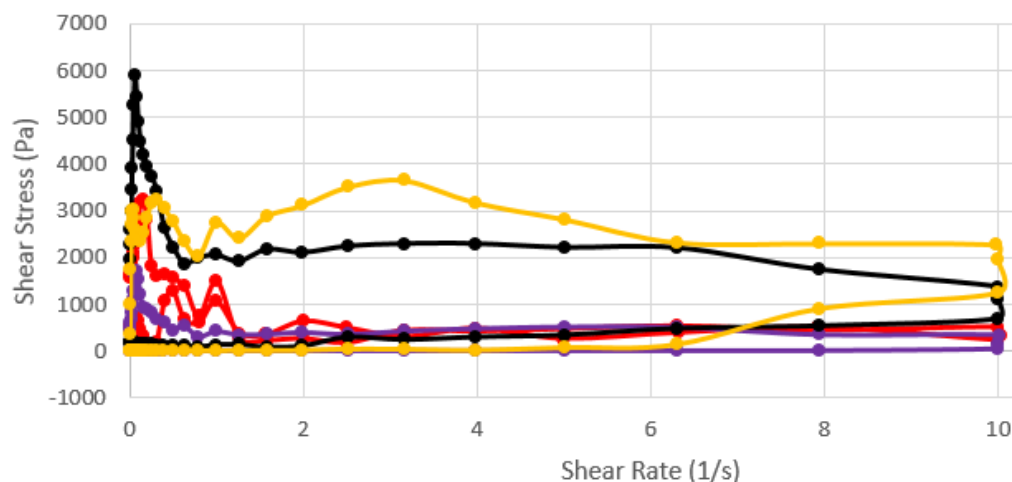


**Figure 44.** Thixotropic loops of the flow rheology analysis for the reference silicone compared to the filled model copolymer materials compounded with HMS-082,  $\text{Pt}(\text{acac})_2$  (250ppm), and DEAD (1:4): Day 0 (●), Day 1 (●), Day 2 (●), and Day 3 (●).

The rheological behavior was similar to that of PDV-0535-Hi-Sil-233D-HMS-151- $\text{Pt}(\text{acac})_2$  at all catalyst concentrations and catalyst to inhibitor ratios.

Figure 45 displays the thixotropic loops of the flow rheology analysis of filled PDV-0535-Hi-Sil-233D-HMS-082- $\text{Pt}(\text{acac})_2$  (250ppm)- DEAD (1:2). The polymer network has started to crosslink because of the heat and pressure from the extruder; this coupled with the deconstruction and reconstruction of the network causes the irregular shape of the loops.

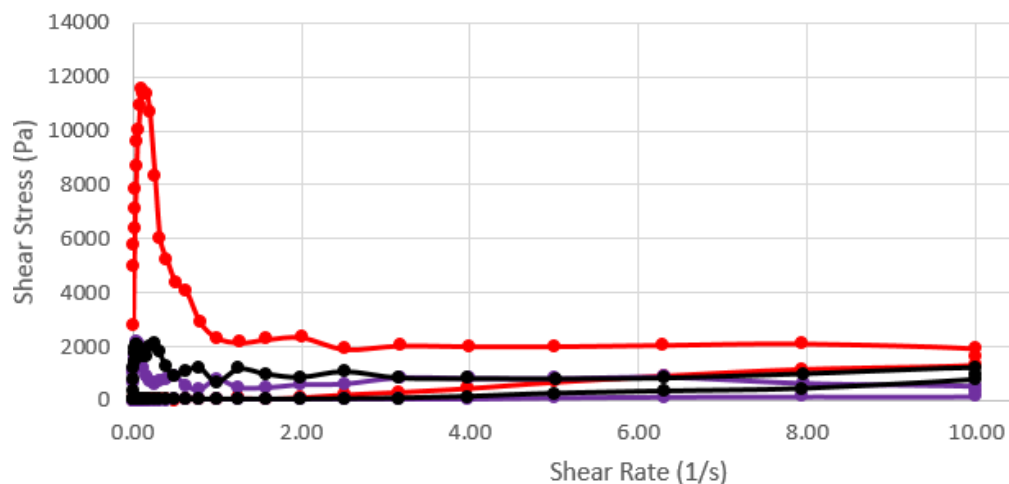


**Figure 45.** Thixotropic loops of the flow rheology analysis for the reference silicone compared to the filled model copolymer materials compounded with HMS-082,  $\text{Pt}(\text{acac})_2$  (250ppm), and DEAD (1:2): Day 0 (●), Day 1 (●), and Day 2 (●).

The rheological behavior was similar to that of PDV-0535-Hi-Sil-233D-HMS-151- $\text{Pt}(\text{acac})_2$  at all catalyst concentrations and catalyst to inhibitor ratios and PDV-0535-Hi-Sil-233D-HMS-082- $\text{Pt}(\text{acac})_2$  (250ppm)- DEAD (1:4).

Figure 46 displays the thixotropic loops of the flow rheology analysis of filled PDV-0535-Hi-Sil-233D-HMS-082- $\text{Pt}(\text{acac})_2$  (125ppm)- DEAD (1:4). The polymer network has started to crosslink because of the heat and pressure from the extruder; this coupled with the deconstruction and reconstruction of the network causes the irregular shape of the loops.

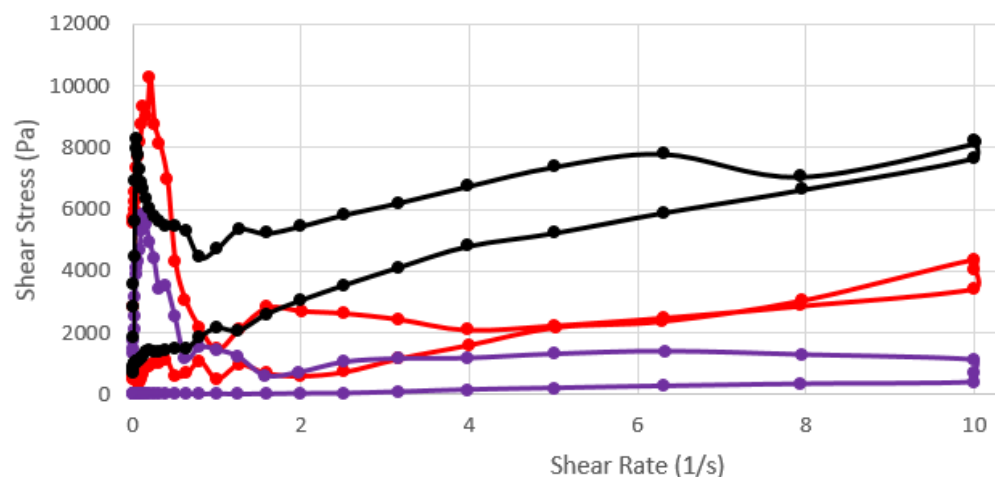


**Figure 46.** Thixotropic loops of the flow rheology analysis for the reference silicone compared to the filled model copolymer materials compounded with HMS-082,  $\text{Pt}(\text{acac})_2$  (125ppm), and DEAD (1:4): Day 0 (●), Day 1 (●), and Day 2 (●).

The rheological behavior was similar to that of PDV-0535-Hi-Sil-233D-HMS-151- $\text{Pt}(\text{acac})_2$  at all catalyst concentrations and catalyst to inhibitor ratios and PDV-0535-Hi-Sil-233D-HMS-082- $\text{Pt}(\text{acac})_2$  samples at 250 ppm catalyst concentration.

Figure 47 displays the thixotropic loops of the flow rheology analysis of filled PDV-0535-Hi-Sil-233D-HMS-082- $\text{Pt}(\text{acac})_2$  (125ppm)- DEAD (1:2).

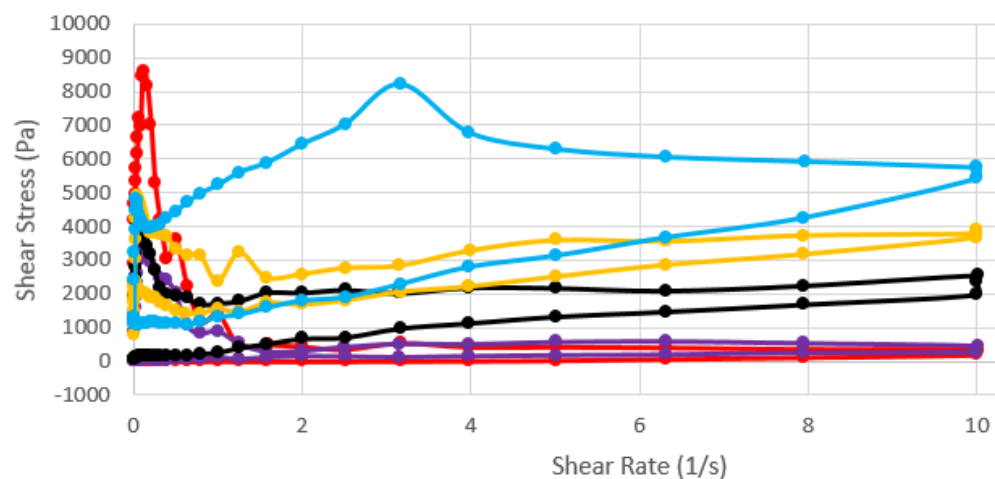


**Figure 47.** Thixotropic loops of the flow rheology analysis for the reference silicone compared to the filled model copolymer materials compounded with HMS-082,  $\text{Pt}(\text{acac})_2$  (125ppm), and DEAD (1:2): Day 0 (●), Day 1 (●), Day 2 (●), Day 3 (●), and Day 4 (●).

The rheological behavior was similar to that of PDV-0535-Hi-Sil-233D-HMS-151-Pt(acac)<sub>2</sub> at all catalyst concentrations and catalyst to inhibitor ratios, PDV-0535-Hi-Sil-233D-HMS-082-Pt(acac)<sub>2</sub> samples at 250 ppm catalyst concentration, and PDV-0535-Hi-Sil-233D-HMS-082-Pt(acac)<sub>2</sub> (125ppm)- DEAD (1:4)

The thermal stability, yield stress, and thixotropic behavior were dependent on the crosslinker used, the catalyst amount and the inhibitor ratio. Both the HMS-151 and HMS-082 with a catalyst amount of 125ppm and 1:2 ratio of inhibitor had the longest shelf stability compared to the other systems. The HMS-082 systems displayed latent curing patterns compared to the HMS-151 systems because of the molecular weight and amount of reaction sites.

## 5.6 Soxhlet extraction analysis of cured material to determine gel content

Each formulation was cured under a UV lamp on two rectangular molds: one that was 0.5cm deep and 3cm deep. The 0.5cm cured materials were used in Soxhlet extraction to determine level of unreacted starting material in each system. The solvent used was THF and each extraction ran for 3 hours. Table 28 displays the percent of crosslinking in the HMS-151 systems.

**Table 28.** Percent of crosslinking of the filled model copolymer compounded with HMS-151 crosslinker.

Polysiloxane	Crosslinking (%)
HMS-151-250ppm-1:4	91
HMS-151-250ppm-1:2	92
HMS-151-125ppm-1:4	92
HMS-151-125ppm-1:2	90

The extraction results showed that each system was able to achieve a 90% or higher amount of crosslinking. This was a sufficient amount of crosslinking to ensure that the final elastomer retained its physical properties and minimal amount of starting

material remained after the vulcanization process. Table 29 displays the percent of crosslinking in HMS-082 systems.

**Table 29.** Percent of crosslinking of the filled model copolymer compounded with HMS-082 crosslinker.

Polysiloxane	Crosslinking (%)
HMS-082-250ppm-1:4	78
HMS-082-250ppm-1:2	84
HMS-082-125ppm-1:4	79
HMS-082-125ppm-1:2	78

Compared to the HMS-151 systems, the HMS-082 systems showed a reduced amount of crosslinking. There are two factors that influence this reduction in crosslinking. The first factor is the concentration of methylhydrosiloxane in HMS-082 compared to HMS-151. This equates to fewer functional sites for crosslinking and an abundance of remaining starting material when crosslinking is completed. The second factor is the molecular weight of the crosslinker. HMS-082 has a molecular weight of 5,500-6,500 g/mol, which is larger than HMS-151 (1,900-2,000 g/mol). The size of the crosslinker causes additional steric hinderance within the system and causes further isolation of reaction sites, preventing further crosslinking.

## 5.7 Dynamic mechanical analysis of cured material

The mechanical properties of crosslinked elastomers were analyzed using dynamic mechanical analysis (DMA) (a.k.a. The Ol' Razzle Dazzle). The 3cm samples were cut into squares and placed into the shear sandwich stage. This geometry was used for its ease of setup and similarity to previous rheological studies of elastomers.<sup>46</sup> The samples were subjected to a constant frequency of 1 Hz/sec. The temperature was set to -130°C and is ramped up at a rate of 5°C/min until 30°C. This sweep shows the storage modulus, loss modulus and tan delta ( $\tan \delta$ ). Of the three, the two that were recorded



were the onset temperature of the storage modulus and the peak temperature of the  $\tan \delta$ . The onset temperature of the storage modulus relates to mechanical failure.  $\tan \delta$  is the midpoint between the glassy and rubbery states, the height and width of the peak is related to the amorphous content of the material.<sup>58</sup> Table 30 shows the onset storage modulus temperature and  $\tan \delta$  of the HMS-151 systems.

**Table 30.** Onset temperature and  $\tan \delta$  of HMS-151 systems.

<b>Polysiloxane</b>	<b>Onset Temperature (°C)</b>	<b>Tan <math>\delta</math> (°C)</b>
HMS-151-250ppm-1:4	-101	-91
HMS-151-250ppm-1:2	-94	-87
HMS-151-125ppm-1:4	-96	-86
HMS-151-125ppm-1:2	-103	-90

The HMS-151 systems do not have a dramatic deviation in temperatures. This indicates that the mechanical properties of each formulation were not significantly affected by amount of catalyst and the ratio of inhibitor. Each formulation increased the  $T_g$  of the polysiloxane by over 20 °C compared to other silicone elastomers because of the bulk of the system.<sup>46</sup>

Table 31 displays the onset storage modulus temperature and  $\tan \delta$  of the HMS-082 systems. As previously mentioned, the crosslinker in these systems has a greater molecular weight but fewer reaction sites.

**Table 31.** Onset temperature and  $\tan \delta$  of HMS-082 systems.

<b>Polysiloxane</b>	<b>Onset Temperature (°C)</b>	<b>Tan <math>\delta</math> (°C)</b>
HMS-082-250ppm-1:4	-96	-87
HMS-082-250ppm-1:2	-95	-85
HMS-082-125ppm-1:4	-96	-86
HMS-082-125ppm-1:2	-100	-87

Just as with the HMS-151, the HMS-082 temperatures had little deviation, showing that the difference in crosslinker had little effect on the mechanical properties. Each formulation from both crosslinkers had an increased  $T_g$  compared to similar silicone

elastomers, as well as similar damping properties.<sup>48</sup> Apart from the increased  $T_g$ , each formulation demonstrated normal storage modulus and  $\tan \delta$  curves when compared to other highly crosslinked silicone elastomers.<sup>46</sup>

## CHAPTER VI

### 6. CONCLUSION

The Process 11 was utilized to successfully compound a model polysiloxane, a silica filler, varied crosslinkers, varied catalysts and an inhibitor at varied ratios to catalyst to produce well-dispersed extrudate materials. The filled materials were characterized by TGA to evaluate the distribution of filler. Oscillatory rheometry was utilized to determine the yield stress and flow rheology was used to evaluate the thixotropic behavior. Once the materials were cured, Soxhlet extraction determined the gel content of the cured elastomers and DMA was utilized to determine the mechanical failure and  $\tan \delta$ . Various formulations with  $\text{Pt}(\text{acac})_2$  were cured and evaluated to characterize these properties.

The first set of experiments compared the effectiveness of two platinum-based catalysts:  $\text{Pt}(\text{acac})_2$  and  $(\text{MeCp})\text{Pt}(\text{Me})_3$ . Each catalyst was used with HMS-151 and HMS-082 crosslinkers at 250ppm and 1:4 ratio with the inhibitor, DEAD. Each formulation was premixed before compounding using the twin screw extruder. TGA, oscillatory rheometry, and flow rheology was performed on each formulation. It was determined that the Process 11 was activating both catalysts by heat generation during compounding that started the crosslinking process. The heat activation of the catalysts shortened the shelf life of the material, regardless of the catalyst in the formulation. This

affected the properties of each formulation. The TGA showed elevated residue levels due to encapsulation of the filled material that prevented volatiles from being released as the crosslinking reaction proceeded over the course of days. The oscillatory rheometry and flow rheology were affected as well. The increasingly crosslinked networks pushed the silica filler aggregates closer together, forming agglomerates and reducing the yield stress and increasing the thixotropic character over time. The (MeCp)Pt(Me)<sub>3</sub> catalyst was determined to be more reactive than the Pt(acac)<sub>2</sub> catalyst. The increased reactivity of the (MeCp)Pt(Me)<sub>3</sub> catalyst shortened the shelf life compared to Pt(acac)<sub>2</sub> and was not suitable for further development of a shelf-stable formulation. For this reason, (MeCp)Pt(Me)<sub>3</sub> was discontinued from further experiments.

Further experiments sought to determine a formulation that would extend shelf stability beyond that of the shelf-life observed in initial experiments with Pt(acac)<sub>2</sub>. The concentration of Pt(acac)<sub>2</sub> and ratios of DEAD to Pt(acac)<sub>2</sub> were varied with the goal of extending the time between compounding and when the material became fully crosslinked. Characterization was performed on each formulation before and after crosslinking. TGA, oscillatory rheometry, and flow rheology were performed on the uncured material, and Soxhlet extraction and DMA analysis was performed on the cured samples.

All the materials that were compounded were clear white, soft, paste-like materials with good dimensional stability. The incorporation of filler enhanced the thermal stability of the materials, but the compounding started the crosslinking reaction prematurely because of the heat and pressure in the extruder. This led to an elevated thermal and rheology data due to the crosslinking. This also had an effect on the shelf

stability of each system. Most of the systems with varied  $\text{Pt}(\text{acac})_2$  concentration and varied ratios of  $\text{Pt}(\text{acac})_2$  to DEAD crosslinked in two days with the exception of two formulations: PDV-0535, Hi-Sil-233D, HMS-151,  $\text{Pt}(\text{acac})_2$  (125ppm), DEAD (1:2); and PDV-0535, Hi-Sil-233D, HMS-082,  $\text{Pt}(\text{acac})_2$  (125ppm), DEAD (1:2). As expected, by reducing the catalyst concentration and increasing the inhibitor to catalyst ratio, shelf stability was increased.

The systems were cured using a UV lamp to create elastomers. These elastomers were analyzed using Soxhlet extraction to determine the amount of uncured starting material that remained in the system. The HMS-082 system had lower percent crosslinking (~78%) due to limited reaction sites along the polymer, the physical size of the crosslinker molecule, and the difficulties with steric hinderance during the crosslinking reaction caused by the size of the crosslinking molecule. HMS-151 systems had similar challenges, but the size of the crosslinker molecule was smaller with more reaction sites, thus allowing more starting material to crosslink (~91%).

DMA was performed on the elastomers to investigate their mechanical properties. Samples from each system analyzed using shear sandwich geometry and was subjected to a constant frequency at a temperature ramp of 5°C/min from -130°C to 30°C. For each system, there was an increase in  $T_g$  compared to other silicone elastomers which is attributed to growing bulk of the system. They also retained similar mechanical failure to one another, showing that there was no practical differences in each formulation from a bulk mechanical standpoint.

## 6.1 Future work

Several challenges were identified over the course of this work that must be overcome to formulate and compound a shelf-stable one-component filled polysiloxane with the ability to be UV-cured on demand. Friction created between the screws and barrel wall of Process 11 and silica filler in the polysiloxane formulation generated heat that activated the catalyst. This catalyst activation was premature and unwanted at this stage of formulation because crosslinking began well before UV-curing was desired. This led to irregular data from all characterization methods.

The main challenge in the formulation was the premature heat activation of the catalyst. The hydrosilylation process is known for being thermally activated.<sup>89</sup> Using different catalysts that are only activated by UV would alleviate this issue. Platinum catalysts are often used with photosensitizers as a way promote UV-activation. An example of a photosensitizer is naphthalene, which improved photopolymerization conversion from 70% to 100%.<sup>89</sup> The thermal properties of the catalyst could also be altered to alleviate heat activation. Some studies have create platinum nitrile complexes that have increased the thermal activation to 80 °C.<sup>90</sup> Those complexes would be ideal for incorporation into formulations that are compounded by twin-screw extrusion. The heat generated by friction between silica and the extruder may be lower than the heat required to activate the catalyst, avoiding premature heat activation of the catalyst and preventing undesirable crosslinking prior to exposure to UV light.

Another alternative is to formulate a two-component formulation. All samples presented in this work were one-component systems. That is, they had all species necessary within the formulation such that the formulation could be removed from the

shelf and UV-cured. In two-component systems of polysiloxane mixtures, the polysiloxane containing the vinyl groups, the filler, and the platinum catalyst are combined in one component and the hydrogen-containing polysiloxane is present in a second component. When the manufacturer or user of the material wants to prepare a cured product, the two components are mixed in specific proportions and the mixture is allowed to cure by the desired mechanism, whether UV-cured or thermally cured.<sup>91</sup> This process prevents the platinum catalyst from interacting with the hydrogen necessary for the hydrosilylation process to begin. The major disadvantage of two-component systems over one-component systems is the extra step of combining components prior to curing.

One way to avoid heat generation during twin-screw extrusion is to avoid the use of twin-screw extrusion all together. While twin-screw extrusion is a very efficient way to compound, the aggressive mixing led to extensive heat generation. High-speed mixers may accomplish sufficient mixing of formulation the components, and disrupt filler agglomerates, while reducing the heat generated during the mixing process. If the heat generated is below the level that is required to activate the catalysts, high-speed mixing could prolong the formulation's shelf stability and result in a material that only cures when exposed to UV light.

Another way to improve upon material characterization and generate more consistent rheological data over the course of curing experiments is to use a photo-curing rheometer for oscillatory rheometry and flow rheology characterization. Using in-situ UV-curing would allow constant monitoring of the effects of curing in real time in one experimental procedure. Individual experiments performed each day proved to be impractical since the rheometer sometimes prevents characterization and important data

is lost when the materials fully crosslinked, rendering them incapable of being analyzed for rheological properties further.



## REFERENCES

1. Dvornic, P. R.; Lenz, R. W. Polysiloxanes. *High Temperature Siloxane Elastomers*; Huthig & Wepf Verlag Basel Publication: New York, 1990; 15-73.
2. Mark, J. E. Physical Properties of Polymers Handbook. *Chapter 54*; Springer Science: New York, 2007; 3-20.
3. Polysiloxanes- by Lachelle Sussman.  
<http://wwwcourses.sens.buffalo.edu/ce435/Polysiloxanes/> (accessed November 2, 2016).
4. Brook, M. A. *Silicon in Organic Organometallic, and Polymer Chemistry*; A Wiley-Interscience Publication: New York, 2000; 1-50.
5. Oberhammer, H.; Boggs, J. E. Importance of (p-d) $\pi$  Bonding in the Siloxane Bond. *J. Am. Chem. Soc.* **1980**, *102*, 7241-7244.
6. Wired Chemist. Common Bond Energies and Bond Lengths.  
[http://www.wiredchemist.com/chemistry/data/bond\\_energies\\_lengths.html](http://www.wiredchemist.com/chemistry/data/bond_energies_lengths.html)  
(accessed March 22, 2017).
7. Momen, G.; Farzaneh, M. Survey of micro/nano filler use to improve silicone rubber for outdoor insulators. *Adv. Mater. Sci.* **2011**, *27*, 1-13.
8. Arrighi, V.; Higgins, J. S.; Burgess, A. N.; Floudas, G. Local dynamics of poly(dimethyl siloxane) in the presence of reinforcing filler particles. *Polymer.* **1998**, *39*, (25), 6369-6376.
9. Sukumar, R.; Menon, A. R. R. Organomodified Kaolin as a Reinforcing Filler for Natural Rubber. *J. Appl. Polym. Sci.* **2007**, *107*, 3476-3483.

10. CABOT. CAB-O-SIL® Fumed Silica for Pharmaceutical and Nutraceutical Applications. file:///C:/Users/Downloads/Brochure-CAB-O-SIL-Fumed-Silica-Pharmaceutical-Nutraceutical-Apps.pdf (accessed February 27, 2017).
11. SIGMA. Fumed Silica. [https://www.sigmaaldrich.com/content/dam/sigma-aldrich/docs/Aldrich/Product\\_Information\\_Sheet/s5130pis.pdf](https://www.sigmaaldrich.com/content/dam/sigma-aldrich/docs/Aldrich/Product_Information_Sheet/s5130pis.pdf) (accessed February 27, 2017).
12. Zhuravlev, L. T. The surface chemistry of amorphous silica. Zhuravlev model. *Colloids Surf., A*. **2000**, 173, 1-38.
13. Chrissafis, K.; Bikiaris, D. Can nanoparticles really enhance thermal stability of polymers? Part I: An overview on thermal decomposition of addition polymers. *Thermochim. Acta*. **2011**, 523, 1-24.
14. Cassagnau, P. Melt rheology of organoclay and fumed silica nanocomposites. *Polymer*. **2008**, 49, 2183-2196.
15. Dorigato, A.; Dzenis, Y.; Pegoretti, A. Filler aggregation as a reinforcement mechanism in polymer nanocomposites. *Mechanics of Materials*, **2013**, 12, 79-90.
16. Chien, A.; Maxwell, R.; Chambers, D.; Balazs, B.; LeMay, J. Characterization of radiation-induced aging in silica-reinforced polysiloxane composites. *Radiat. Phys. Chem.* **2000**, 59, 493-500.
17. Schwenker, K. W. 2017.
18. Dorigato, A.; Pegoretti, A.; Penati, A. Linear low-density polyethylene/silica micro- and nanocomposites: dynamic rheological measurements and modelling. *eXPRESS Polymer Letters*, **2010**, 4, (2), 115-129.

19. Raghavan, S. R.; Riley, M. W.; Fedkiw, P. S.; Khan, S. A. Composite Polymer Electrolytes Based on Poly(ethylene glycol) and Hydrophobic Fumed Silica: Dynamic Rheology and Microstructure. *Chem. Mater.* **1998**, *10*, (1), 244-251.
20. Luginsland, H-D.; Frohlich, J.; Wehmeier, A. Influence of different silanes on the reinforcement of silica-filled rubber compounds. *Rubber Chemistry and Technology*, **2002**, *75*, 563-579.
21. Shim, S. E.; Isayev, A. I. Rheology and structure of precipitated silica and poly(dimethyl siloxane) system. *Rheologica Acta*, **2004**, *43*, 127-136.
22. Burnside, S. D.; Giannelis, E. P. Synthesis and Properties of New Poly(Dimethylsiloxane) Nanocomposites. *Chem. Mater.* **1995**, *7*, (9), 1597-1600.
23. Verdejo, R.; Barroso-Bujans, F.; Rodriguez-Perez, M. A.; de Saja, J. A.; Lopez-Manchado, M. A. Functionalized graphene sheet filled silicone foam nanocomposites. *J. Mater. Chem.* **2008**, *18*, 2221-2226.
24. Kim, H.; Lee, B.; Choi, S.; Kim, S.; Kim, H. The effect of types of maleic anhydride-grafted polypropylene (MAPP) on the interfacial adhesion properties of bio-flour-filled polypropylene composites. *Composites Part A: Applied Science and Manufacturing*. **2007**, *38*, 1473-1482.
25. Beyer, G. Nanocomposites: a new class of flame retardants for polymers. *Plastics, Additives and Compounding*. **2002**, *4*, (10), 22-28.
26. Dorigato, A.; Pegoretti, A.; Frache, A. Thermal stability of high density polyethylene–fumed silica nanocomposites. *J. Therm. Anal. Calorim.* **2012**, *109*, 863-873.

27. D' Amato, M.; Dorigato, A.; Fambri, L.; Pegoretti, A. High performance polyethylene nanocomposite fibers. *eXPRESS Polymer Letters*. **2012**, *6*, (12), 954-964.
28. Zhang, Q.; Archer, L. A. Poly(ethylene oxide)/Silica Nanocomposites: Structure and Rheology. *Langmuir*. **2002**, *18*, (26), 10435-10442.
29. Raghavan, S. R. Rheology of Silica Dispersions in Organic Liquids: New Evidence for Solvation Forces Dictated by Hydrogen Bonding. *Langmuir*, **2000**, *16*, (21), 7920-7930.
30. Wang, Y.; Wang, J. Shear Yield Behavior of Calcium Carbonate-Filled Polypropylene. *Polym. Eng.Sci.* **1999**, *39*, (1), 190-198.
31. Le Meins, J.; Moldenaers, P.; Mewis, J. Suspensions in Polymer Melts. 1. Effect of Particle Size on the Shear Flow Behavior. *Ind. Eng. Chem. Res.* **2002**, *41*, (25), 6297-6304.
32. Vermant, J. Quantifying dispersion of layered nanocomposites via melt rheology. *J. Rheol.* **2007**, *51*, 429-450.
33. Ibaseta, N.; Biscans, B. Fractal dimension of fumed silica: Comparison of light scattering and electron microscope methods. *Powder Technol.* **2010**, *203*, 206-210.
34. Bose, S.; Mahanwar, P. A. Influence of particle size and particle size distribution on MICA filled nylon 6 composite. *J. Mater. Sci.* **2005**, *40*, 6423-6428.
35. Thomas, T. P.; Kuruvilla, J.; Sabu, T. Mechanical properties of titanium dioxide-filled polystyrene microcomposites. *Mater. Lett.* **2003**, *58*, 281-289.

36. Jamil, M. S.; Ahmad, I.; Abdullah, I. Effects of Rice Husk Filler on the Mechanical and Thermal Properties of Liquid Natural Rubber Compatibilized High-Density Polyethylene/Natural Rubber Blends. *Journal of Polymer Research*. **2006**, *13*, 315-321.
37. DeGroot, Jr., J. V.; Macosko, C. W. Aging Phenomena in Silica-Filled Polydimethylsiloxane. *J. Colloid Interface Sci.* **1999**, *217*, 86-93.
38. Sombatsompop, N.; Thongsang, S.; Markpin, T.; Wimolmala, E. Fly Ash Particles and Precipitated Silica as Fillers in Rubbers. I. Untreated Fillers in Natural Rubber and Styrene–Butadiene Rubber Compounds. *J. Appl. Polym. Sci.* **2004**, *93*, 2119-2130
39. Wei, L.; Hu, N.; Zhang, Y. Synthesis of Polymer—Mesoporous Silica Nanocomposites. *Materials*. **2010**, *3*, 4066-4079.
40. PolyOne. What is a TPE? <http://www.polyone.com/products/thermoplastic-elastomers/tpe-knowledge-center/tpe-faqs> (accessed Nov 8, 2016).
41. Britannica, T. E. of E. Charles Goodyear  
<https://www.britannica.com/biography/Charles-Goodyear> (accessed July 20, 2018).
42. Chen, J.; Lv, Q.; Wu, D.; Yao, X.; Wang, J.; and Li, Z. Nucleation of a Thermoplastic Polyester Elastomer Controlled by Silica Nanoparticles. *Indust. Eng. Chem. Res.* **2016**, 5279-5286.
43. Norton, J. Crosslinking Powerpoint, 2014.
44. Polmanteer, K. E.; Koch, R. J. *Rubber Chemistry and Technology* **1957**, *30* (2), 406–418.

45. Ray, C. So, which is better, Platinum or Peroxide?  
<https://www.tblplastics.com/platinum-vs-peroxide-silicone-tubing/> (accessed Nov 13, 2019).
46. Menard, K. P. *Dynamic mechanical analysis: a practical introduction*; CRC Press: Boca Raton, FL, 2008.
47. Dunson, D. Characterization of Polymers using Dynamic ...  
<https://www.eag.com/wp-content/uploads/2017/09/M-022717-Characterization-of-Polymers-using-Dynamic-Mechanical-Analysis.pdf> (accessed Nov 15, 2019).
48. Menard, K. P.; Menard, N. R. *Encyclopedia of Polymer Science and Technology* **2015**, 1–33.
49. Thermo Electron Corporation. Short introduction into rheology.  
<https://www.scribd.com/presentation/161088307/Basics-Rot-Creep-Osc> (accessed March 5, 2017).
50. Gelest. Contact Us. <http://www.gelest.com/contact-us/> (accessed on October 14, 2016).
51. PPG. Contact. <http://corporate.ppg.com/Contact.aspx> (accessed on October 14, 2016).
52. ThermoFisher Scientific. About Us. <http://corporate.thermofisher.com/en/about-us.html> (accessed on May 17, 2016).
53. Thermo Fisher Scientific. Process 11 Parallel Twin-Screw Extruder.  
<https://www.thermofisher.com/order/catalog/product/567-7600> (accessed on October 23, 2016).

54. KitchenAid. Contact Us. <http://www.kitchenaid.com/contact-us/> (accessed on October 17, 2016).
55. TA Instruments. TA Directory. <http://www.tainstruments.com/contact/ta-directory/> (accessed on May 17, 2016).
56. SunRay - High-Power UV Flood Curing Lamp.  
<https://www.uvitron.com/products/floods/sunray.php> (accessed Jun 11, 2019).
57. Principle of Soxhlet extraction and Experimental Setup of Soxhlet Extractor.  
<http://oleoresins.melbia.com/principle-of-soxhlet-extraction-and-experimental-setup.html> (accessed Nov 14, 2019).
58. Geiger, M. Introduction to Dynamic Mechanical Testing for Rubbers and Elastomers, 2017.
59. Jovanovic, J. D.; Govrdarica, M. N.; Dvornic, P. R.; Popovic, I.G. The thermogravimetric analysis of some polysiloxanes. *Polym. Degrad. Stab.* **1998**, *61*, 87-93.
60. Ahmad, S.; Gupta, A. P.; Sharmin, E.; Alam, M.; Pandey, S. K. Synthesis, characterization and development of high performance siloxane-modified epoxy paints. *Prog. Org. Coat.* **2005**, *54*, 248-255.
61. Camino, G.; Lomakin, S. M.; Lageard, M. Ballistreri, A.; Garozzo, D.; Montaudo, G. Thermal polydimethylsiloxane degradation. Part 2. The degradation mechanisms. *Polymer.* **2002**, 2011-2015.
62. Ramirez, I.; Jayaram, S.; Cherney, E. A.; Gauthier, M.; Simon, L. Erosion Resistance and Mechanical Properties of Silicone Nanocomposite Insulation. *IEEE Transactions on Dielectrics and Electrical Insulation.* **2009**, *16*, (1), 52-59.

63. Lauter, U.; Kantor, S. W.; Schmidt-Rohr, K.; MacKnight, W. J. Vinyl-Substituted Silphenylene Siloxane Copolymers: Novel High-Temperature Elastomers. *Macromolecules*. **1999**, *32*, 3426-3431.
64. Chenoweth, K.; Cheung, S.; van Duin, A. C.; Goddard III, W. A.; Kober, E. M. Simulations on the Thermal Decomposition of a Poly(dimethylsiloxane) Polymer Using the ReaxFF Reactive Force Field. *J. Am. Chem. Soc.* **2005**, *127* (19), 7192-7202.
65. Ballistreri, A.; Garozzo, D.; Montaudo, G. Mass Spectral Characterization and Thermal Decomposition Mechanism of Poly(dimethylsiloxane). *Macromolecules*. **1984**, *17* (7), 1312-1315
66. Sunan, T.; Damrongsakkul, S.; Hemvichian, K. Rimdusit, S. Thermal degradation behaviors of polybenzoxazine and silicon-containing polyimide blends. *Polym. Degrad. Stab.* **2007**, *92*, 1265-1278.
67. Schiavon, M. A.; Redondo, S. U. A.; Pina, S. R. O. Yoshida, I. V. P. Investigation on kinetics of thermal decomposition in polysiloxane networks used as precursors of silicon oxycarbide glasses. *J. Non-Crystal. Solids*. **2002**, *304*, 92-100.
68. Lewicki, J. P.; Liggat, J. J.; Patel, M. The thermal degradation behaviour of polydimethylsiloxane/montmorillonite nanocomposites. *Polym. Degrad. Stab.* **2009**, *94*, 1548-1557.
69. Mazhar, M.; Zulfiqar, M.; Piracha, A.; Ali, S.; Ahmed, A. Comparative Thermal Stability of Homopolysiloxanes and Copolysiloxanes of Dimethyl/Diphenyl Silanes. *J. Chem. Soc. of Pak.* **1990**, *12* (3), 225-229.



70. Deshpande, G.; Rezac, M. E. Kinetic aspects of the thermal degradation of poly(dimethylsiloxane) and poly(dimethyl diphenyl siloxane). *Polym. Degrad. Stab.* **2001**, *76*, 17-24.
71. Reynaud, E.; Jouen, T.; Gauthier, C.; Vigier, G.; Varlet, J. Nanofillers in polymeric matrix: a study on silica reinforced PA6. *Polymer*. **2001**, *42*, 8759-8768.
72. Dey, T. K.; Tripathi, M. Thermal properties of silicon powder filled high-density polyethylene composites. *Thermochim. Acta*. **2010**, *502*, 35-42.
73. Laachachi, A.; Coches, M.; Ferriol, M.; Lopez-Cuesta, J. M.; Leroy, E. Influence of TiO<sub>2</sub> and Fe<sub>2</sub>O<sub>3</sub> fillers on the thermal properties of poly(methyl methacrylate) (PMMA). *Mater. Lett.* **2005**, *59*, 36-39.
74. Chien, A.; Maxwell, R. S.; DeTeresa, S.; Thompson, L.; Cohenour, R.; Balazs, B. The Effect of Filler-Polymer Interactions on Cold-Crystallization Kinetics in Crosslinked, Silica Filled PDMS/PDPS Copolymer Melts. *J. Polym. Sci., Part B: Polym. Phys.* **2006**, *44*, 1898-1906.
75. Wypych, G. *Handbook of Curatives and Crosslinkers*; ChemTec Publishing, 2019.
76. Erkens, I. J. M. (2014). Understanding and controlling atomic layer deposition of platinum and platinum oxide. Eindhoven: Technische Universiteit Eindhoven, 2014
77. Pedrazzoli, D.; Dorigato, A.; Pegoretti, A. Monitoring the Mechanical Behaviour of Electrically Conductive Polymer Nanocomposites Under Ramp and Creep

- Conditions. *Journal of Nanoscience and Nanotechnology*. **2012**, 12, (5), 4093-4102.
78. Wiswall, J. T.; Wooldridge, M. S.; Im, H. G. An experimental investigation of catalytic oxidation of propane using temperature controlled Pt, Pd, SnO<sub>2</sub>, and 90% SnO<sub>2</sub>–10% Pt catalysts.  
<https://pubs.rsc.org/en/content/articlelanding/2013/cy/c2cy20512b#!divAbstract> (accessed Nov 15, 2019).
79. Marchi, S.; Sangermano, M.; Meier, P.; Kornmann, X. A Comparison of the Reactivity of Two Platinum Catalysts for Silicone Polymer Cross-Linking by UV-Activated Hydrosilation Reaction. *Macromolecular Reaction Engineering* **2015**, 9 (4), 360–365.
80. Zhu, Z.; Thompson, T.; Wang, S.; von Meerwall, E. D.; Halasa, A. Investigating Linear and Nonlinear Viscoelastic Behavior Using Model Silica-Particle-Filled Polybutadiene. *Macromolecules*. **2005**, 38, (21), 8816-8824.
81. Ghezzehei, T. A.; Or, D. Rheological Properties of Wet Soils and Clays under Steady and Oscillatory Stresses. *Soil Sci. Soc. Am. J.* **2001**, 65, 624-637.
82. Prashantha, K.; Soulestin, J.; Lacrampe, M. F.; Krawczak, P.; Dupin, G.; Claes, M. Masterbatch-based multi-walled carbon nanotube filled polypropylene nanocomposites: Assessment of rheological and mechanical properties. *Compos. Sci. Technol.* **2009**, 69, 1756-1763.
83. Chen, P.; Zhang, J.; He, J. Increased Flow Property of Polycarbonate by Adding Hollow Glass Beads. *Polym. Eng. Sci.* **2005**, 45, (8), 1119-1131.

84. Lee, C. H.; Moturi, V.; Lee, Y. Thixotropic property in pharmaceutical formulations. *J. Controlled Release*. **2009**, *136*, 88-98.
85. Giuseppe, E. D.; Davaille, A.; Mittelstaedt, E.; François, M. Rheological and Mechanical Properties of Silica Colloids: from Newtonian Liquid to Brittle Behaviour. *Rheologica Acta* **2012**, *51* (5), 451–465.
86. Galgali, G.; Ramesh, C.; Lele, A. A Rheological Study on the Kinetics of Hybrid Formation in Polypropylene Nanocomposites. *Macromolecules*. **2001**, *34*, (4), 852-858.
87. Weiss, K. D.; Carlson, D.; Nixon, D. A. Viscoelastic Properties of Magneto- and Electro-Rheological Fluids. *Journal of Intelligent Material Systems and Structures*. **1994**, *5*, 772-775.
88. Planes, E.; Chazeau, L.; Vigier, G.; Stuhldreier, T. Influence of silica fillers on the ageing by gamma radiation of EDPM nanocomposites. *Compos. Sci. Technol.* **2006**, 1-23.
89. Xi, L.; Liu, Z.; Su, J.; Bei, Y.; Xiang, H.; Liu, X. UV-Activated Hydrosilylation of (Me-Cp)Pt(Me)<sub>3</sub> : Enhanced Photocatalytic Activity, Polymerization Kinetics, and Photolithography. *Journal of Applied Polymer Science* **2019**, *136* (47), 48251.
90. Islamova, R.; Dobrynin, M.; Ivanov, D.; Vlasov, A.; Kaganova, E.; Grigoryan, G.; Kukushkin, V. Bis-Nitrile and Bis-Dialkylcyanamide Platinum(II) Complexes as Efficient Catalysts for Hydrosilylation Cross-Linking of Siloxane Polymers. *Molecules* **2016**, *21* (3), 311.

91. Schlak, O; Michel, W.; Munchenbach, B. Thermosetting Organopolysiloxane Mixtures Containing Platinum Catalyst Dispersed in Solid Silicone Resin. U. S. Patent 4,481,341, November 6, 1984.